ATTACHMENT 4

PROJECTED RT_{PTS} REVISION

Consumers Power Company
Palisades Plant
Docket 50-255

WESTINGHOUSE CORPORATION TOPICAL REPORT WCAP 13348

PALISADES NUCLEAR PLANT REACTOR VESSEL FLUENCE ANALYSIS
May 1992

WESTINGHOUSE CLASS 3

WCAP-13348

Consumers Power Company
Palisades Nuclear Plant
Reactor Vessel Fluence Analysis

E. P. Lippincott
May 1992

APPROVED: F. L. Lau

F. L. Lau, Manager
Radiation Engineering and Analysis

Prepared by Westinghouse for the Consumers Power Company
Purchase Order DTE-91438
Work performed under Shop Order No. MOZP-450A

WESTINGHOUSE ELECTRIC CORPORATION
Energy Systems Business Unit
P.O. Box 355
Pittsburgh, Pennsylvania 15230

Consumers Power Company Palisades Nuclear Plant

Reactor Vessel Fluence Analysis

Table of Contents

List of Tables

List of Figures

1. Introduction

In order to evaluate the condition of reactor vessel pressure vessels and assure continued safe operation, it is necessary to determine the amount of embrittlement that occurs due to exposure to the radiation field. Accurate assessment of the vessel exposure will help to assure that the reactor can be operated in the least restrictive mode possible with respect to:

1 - 10CFR50 Appendix G pressure/temperature limit curves for normal heatup and cooldown of the reactor coolant system;

2 - Emergency Response Guideline (ERG) pressure/temperature limit curves; and

3 - Pressurized Thermal Shock (PTS) RT_{PTS} screening criteria.

In addition, an accurate measure of the neutron exposure of the reactor vessel and support structure can provide a sound basis for requalification should operation of the plant beyond the current design and/or licensed lifetime prove to be desirable.

The radiation damage to the vessel is primarily caused by high energy neutrons which originate from fission occurring in the fuel region. A small fraction of the fission neutrons manage to escape from the core and impinge on the vessel steel. Within the nuclear industry it has been common practice (cf. ASTM Standard E560 [1]) to base estimates of the fast neutron exposure of reactor vessels either (1) directly on the results of neutron transport calculations or (2) on the analytical results normalized to measurements obtained from internal surveillance capsules, or, more recently from ex-vessel dosimetry. However, there are potential drawbacks associated with both of these approaches to exposure assessment.

In performing neutron transport calculations for pressurized water reactors, several design and operational variables have an impact on the magnitude of the analytical prediction of exposure rates within the reactor vessel wall, as well as on the uncertainties associated with that prediction. Dimensions of the reactor internals and reactor vessel are especially important and differences between design and as-built dimensions may exist. Errors in the exact distance from the core region to the vessel may lead to a consistent, plant specific bias in the calculational results. Examples of operational variables that may affect calculational accuracy are cycle-to-cycle variations in core power and fuel burnup distributions (especially with implementation of low leakage loading patterns and other fuel management schemes designed to reduce vessel exposure at critical points), and variations of water temperature in the downcomer regions of the

reactor internals. Treatment of these important variables in the analysis using a methodology relying on plant-specific calculations, with benchmarking to in-vessel and ex-vessel neutron flux measurements, will lead to an increased confidence and decreased uncertainty in the exposure evaluations for the reactor vessel.

Uncertainties in the reactor vessel fluence evaluation also arise from the model approximations and nuclear data errors that are integral to any transport calculation. Due to computer limitations, the calculations are carried out in two dimensions and have a finite number of spatial points to represent the geometry. In addition, limits are also placed on the number of scattering angles and the number of neutron energy groups. Of major importance are cross section uncertainties that can have large impacts on the transport of neutrons through the region from the fuel to the reactor cavity, and uncertainties on the neutron source distribution and magnitude. The existence of these uncertainties, together with the plant specific uncertainties in dimensions of reactor components, requires that the calculations be validated by comparison to measured results, both related controlled benchmarks (such as the those measured under the NRC-sponsored Light Water Reactor Pressure Vessel Surveillance Dosimetry Improvement Program (LWR-PV-SDIP) [2]), and, most importantly, plant specific measurements at Palisades.

The Westinghouse calculational methodology [3] has been benchmarked against a number of relevant LWR benchmarks including the PCA at ORNL [4], the VENUS mockup at Mol, Belgium [5], and the H. B. Robinson PWR [6], as well as against a large database of reactor surveillance capsule measurements and reactor cavity dosimetry measurements [3],[7],[8]. These benchmarking efforts have successfully identified biases that exist in the calculations and pointed the way to investigate the causes of these biases. However, further work remains to be done to complete the understanding of the biases in key parameters that are input to the calculations and to make the needed corrections to these parameters to eliminate the bias contribution (i.e. develop and test improved cross section evaluations).

The uncertainties in the transport calculation of vessel fluence ($E > 1$ MeV) (without inclusion of plant specific dosimetry results) are generally estimated to be in the range of 15 to 20% (1σ) [4],[10],[11],[9]. Data bases of plant specific measurements support this uncertainty assessment since almost all C/M ratios fall between 0.7 and 1.3 ($\pm 2\sigma$ bounds) [3]. These calculational uncertainties are large enough that the plant specific measurements can, in general, provide a noticeable improvement in vessel fluence accuracy. In addition, the measurements provide confidence that biases as large as 15-20% can be recognized and eliminated from the fluence predictions. For example, such biases could occur from unknown errors in reactor parameters or from unknown correlations in these errors.

The most extensive efforts so far to quantitatively evaluate the calculational bias in PWR geometries have been made by Maerker and others at ORNL [10],[11] using the LEPRICON code [12]. These efforts have resulted in an improved knowledge of uncertainty estimates for a variety of calculational parameters, and specific results from the LEPRICON studies can be applied in a generic fashion to give approximate indications of uncertainties of best estimate exposure evaluations. However, due to the many unknowns in actual uncertainties of the input data and the relation (covariances) between these uncertainties, and also the deviation of the probability distributions from the usually assumed normal curve, the LEPRICON procedure does not yet give an uncertainty derivation that can be totally relied upon. Therefore, the LEPRICON results by themselves cannot be used conclusively to determine the quantitative real changes in parameters. The LEPRICON analysis does produce parameter changes by least squares unfolding that provide indications of which parameters are likely to be the significant causes of bias.

The LEPRICON results have demonstrated that the measured values of reaction rates from internal capsules and from ex-vessel (cavity) dosimetry can be used to adjust the calculation of vessel exposure and thereby largely eliminate bias that exists in the calculation. In particular, bias in calculation of the neutron transport from the core through vessel internals and water regions can be disregarded when appropriate measurements are available. This method in effect reduces the region of concern to the smaller volume between the capsules and the cavity, and eliminates significant uncertainty arising from the treatment of the neutron source (both fission spectrum and source distribution uncertainties) and transport of the neutrons from the core to the vessel and capsule measurement points.

Derivation of fluence estimates from plant specific measurements involves several steps. The measurements consist of reactions that occur in dosimeters. Each of these reactions samples the flux of neutrons impingent on the detector with a probability given by the reaction cross section. The actual reaction measured then represents a test of the calculation at the measurement point, but does not provide a complete measure of the desired exposure parameters related to neutron embrittlement. In addition, the evaluation of the fluence at the reactor vessel involves an interpolation or extrapolation in space from the measurement points and usually also involves an extrapolation in time to integrate the total exposure. For these reasons the measurements by themselves do not determine the vessel exposure but when used in concert with the calculations produce a more accurate best-estimate neutron fluence.

Typical absolute uncertainties in individual reaction rate measurements are 5 to 10% (note that the measurement precision is better, typically in the 1-3% range), when properly calibrated and benchmarked. These uncertainties have been verified by round-

robin testing [13] and by considerable efforts to tie results to standards through the National Institute of Standards and Technology (NIST).

In view of the many variables involved and the lack of knowledge of the detailed probability distributions of all of these variables, it is apparent that a completely rigorous definition of the true uncertainty in the evaluated fluence is not possible for the present state of the art. However, it is possible to look at the effect of each of the major known uncertainties that enter the evaluation. These are considered individually in this report and conservative estimates of the uncertainty contributions are determined. By combining the uncertainties, a conservative limit can be placed on the uncertainty in the fluence values used for assessment of vessel condition. This assessment is shown to be consistent with the general expectations described above.

2. Calculation of Fluence

The Palisades reactor vessel fluence calculations were carried out using techniques that have been applied by Westinghouse to a large number of other reactors for surveillance capsule analyses and vessel fluence evaluation [3]. Uncertainties in the reactor vessel fluence evaluation arise from the approximations and data errors that are an integral part of any transport calculation. A detailed evaluation of the calculational uncertainties is given in Section 2.2.

The existence of the inherent calculational uncertainties, together with plant-specific reactor geometry uncertainties, requires that the calculations be benchmarked to measured results, both related controlled benchmarks (such as the those measured under the NRC-sponsored LWR Pressure Vessel Surveillance Dosimetry Improvement Program (LWR-PV-SDIP) [14]), and plant specific measurements at Palisades (discussed below). The Westinghouse methodology has been benchmarked against a number of benchmarks including the PCA at ORNL [4], the VENUS mockup at Mol, Belgium [5], and the H. B. Robinson PWR [6], as well as against a large database of reactor surveillance capsule measurements and reactor cavity dosimetry measurements [7],[8]. These benchmark calculations support the accuracy of the methods and cross sections, especially in the interpolation of the results between the capsules and the cavity to get the fluence throughout the vessel. However, the benchmark results of most significance for establishing the accuracy of the Palisades calculated fluence results are measurements made in the Palisades plant itself. Such measurements serve not only to check the calculational accuracy, but also provide a check on plant specific parameters such as actual geometry, material densities, and neutron source distributions.

2.1 Palisades Calculations

In the present analysis calculations have been performed to evaluate the Palisades reactor vessel fast neutron exposure through cycle 9 (ended February 1992). The analysis was carried out to determine average flux values for cycles 1 to 5 and for cycles 6 to 7. Previous calculations reported for cycle 8 [15] and for cycle 9 [16] were utilized to integrate the flux through the end of cycle 9. All calculations were performed using consistent analysis procedures as described below.

The fast neutron exposure calculations for the reactor and cavity geometry were carried out using discrete ordinates transport techniques. These calculations provided the energy distribution of neutron flux for use in determining the actual exposure at key locations in the reactor vessel wall. The calculations all use an improved methodology that takes into account the irregular spacing of the Palisades fuel assemblies and the effect of the fuel burnup for each assembly on the neutron source from that assembly. Thus these

calculations represent an update of calculations previously reported for the average flux over Cycles 1-5 [17] and for Cycles 1-7 average [18]. The calculation reported in reference [15] is also an update of the Cycle 8 calculation reported in reference [18].

A plan view of the calculational model of the reactor geometry at the core midplane elevation is shown in Figures 2-1 and 2-2. Due to the radial extent of the geometry modelled and in order to keep a fine spatial mesh definition, the calculation was carried out in two parts as shown in these figures. The inner part of the model encompassed the fuel region and the ex-core region through the water inside the reactor vessel. This part of the model contained 61 azimuthal mesh and 85 radial mesh. The outer part of the model utilized the boundary source calculated in the inner part of the model at the inside of the core barrel to calculate the neutron transport from the barrel through the reactor vessel and cavity and into the biological shield. The outer part of the model contained 83 radial mesh. The overlap of the inner and outer parts of the model was found to be sufficient so that negligible error was introduced by splitting the calculation into the two parts.

Since the reactor exhibits 1/8 core symmetry, a 0 to 45 degree sector with reflecting boundaries is modeled, as depicted in the figures. In addition to the core, reactor internals, reactor vessel, and the primary biological shield, the model also included explicit representations of a surveillance capsule attached to the vessel wall at 20 degrees, the vessel cladding, and the reflective insulation located external to the vessel. From a neutron transport standpoint, the inclusion of the surveillance capsules and associated support structures in the analytical model is significant for analysis of capsule dosimetry results and evaluation of capsule exposures. To a lesser extent, the capsule impacts the reactor vessel exposure at locations close to the capsule. Inclusion of the surveillance capsule also allowed a comparison of the new calculated flux value in the capsule for Cycles 1-5 with the W-290 capsule exposure result, and provided a neutron spectrum at the capsule center for evaluation of the measurements.

The transport calculation for each of the two parts of the reactor model depicted in Figures 2-1 and 2-2 was carried out in R,θ geometry using the DOT-IIIW two-dimensional discrete ordinates transport theory code [19] and the SAILOR cross-section library [20]. The SAILOR library is a 47 neutron energy group ENDF-B/IV based data set produced specifically for light water reactor applications. In these analyses, anisotropic scattering was treated with a P_3 expansion of the cross-sections and the angular discretization was modeled with an S_8 order of angular quadrature. The calculation was normalized to the axial peak power location and for operation at a thermal power level of 2530 MW.

Figure 2-1

Reactor Geometry Showing a 45° R,θ Sector
For the Inner Part of the Model

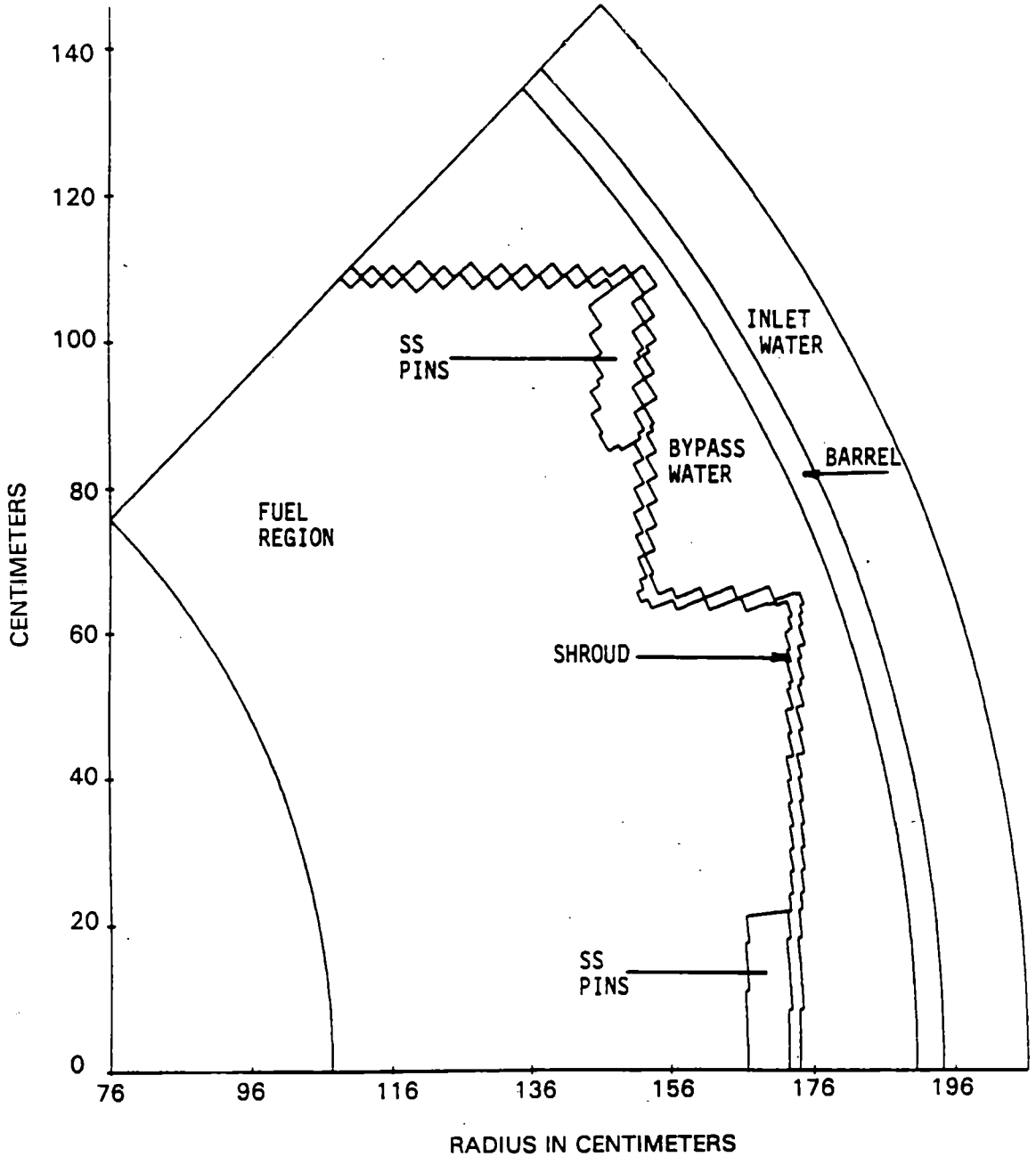

Figure 2-2

Reactor Geometry Showing a 45° R,θ Sector
For the Outer Part of the Model

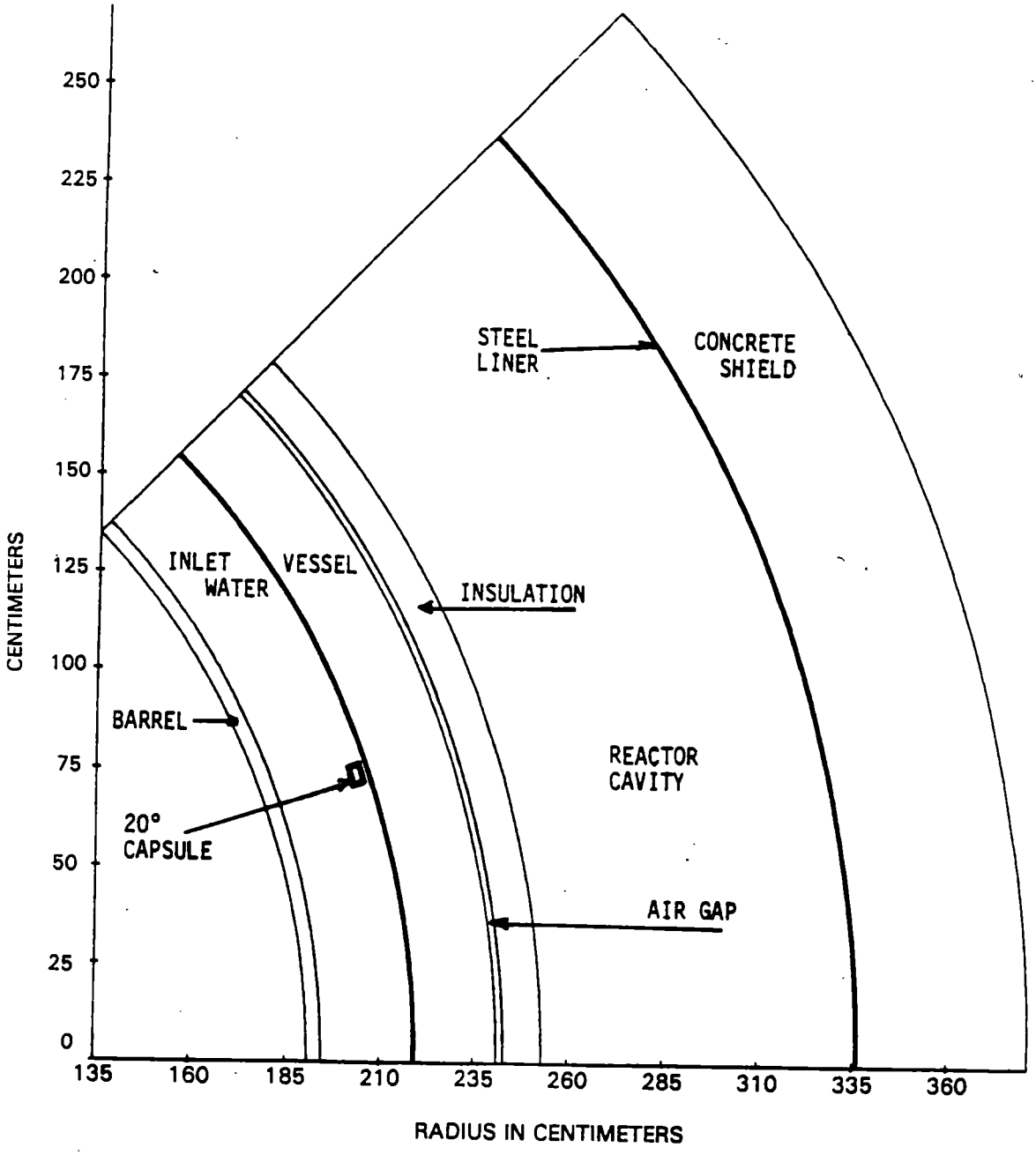

The SAILOR library was chosen because of the extensive testing of this set for application in LWR environments. It is recognized that improved cross section sets have been developed and are currently being tested [21]. In particular, the ENDF/B-VI cross section for iron inelastic scattering has been modified to better fit data that indicates increased transmission of high energy neutrons. Use of the modified iron cross section would result in a small increase in the calculated flux inside the vessel and a larger increase in the calculated response of dosimetry located in the cavity. The resultant decrease in the calculated ratio of flux at the inside of the vessel to the cavity dosimetry response will therefore result in lower projected vessel fluences when cavity dosimetry results are used to extrapolate back. Thus, the SAILOR cross section set will give conservative results for the vessel when cavity dosimetry results are applied. In addition, it should be noted that this cross section change does not appreciably affect the transmission of neutrons near 1 MeV through iron, and, as a result, calculations of neutron flux ($E > 1$ MeV) transmission through the vessel indicate a smaller effect than the change in reaction rates [21].

The spatial core power distributions utilized in the calculations were supplied by Consumers Power [22]. They were used to determine the neutron source time-averaged over the actual operation period for each calculation. The power distribution was supplied as a pin-by-pin power distribution for each of the outer assemblies and as cycle burnups for each assembly. The neutron source was derived for each fuel pin and for each fuel assembly using burnup dependent values of the fission neutron energy spectrum, neutrons per fission, and energy per fission. The source spectrum was calculated by determining the fraction of fissions occurring in each of the important uranium and plutonium isotopes for the mid-cycle burnup and calculating a resultant average fission spectrum using the ENDF-B/V fission spectrum for each isotope. Axial peaking factors were also entered for each assembly. Since almost all the assemblies peaked near the same axial height, the peak power for all assemblies was used, and the calculation therefore represents the fluence at the maximum axial point as if the entire core was at that peak power. This conservative assumption results in calculated flux values that are indicated to be high by as much as 4% at the axial midplane location. The source from each assembly was spatially located to take into account the varying gaps between fuel assemblies and thus represents the location of source from each pin accurately.

The source was converted from the X-Y pin geometry to the R-θ DOT geometry by distributing the source over a square area equal to the pitch for each pin. This pin area was then divided into a 10 x 10 array, and each of these 100 source area elements per pin was placed into the DOT mesh containing the center point of the source area element. The error in source positioning, both radial and azimuthal, was thus kept to less than ± 0.07 cm for each of these source area elements. Averaging the error over the very

large number of source area elements (100 area elements per pin times 225 pins per assembly times the assemblies included in the model) produces an extremely small resultant bias in source positioning. Thus the source location error due to the geometry conversion can be assumed to be negligible. The neutron source was input to the DOT calculation for the inner part of the model as a 47 group fixed source for each DOT spatial mesh point in the fuel region.

Details of fuel assembly locations, core geometry, and other reactor parameters were taken from the information supplied by Consumers Power for the Cycle 8 calculation [23]. Values of water temperature were slightly different in Cycle 8 and the normal values were used for the other cycles.

2.2 Calculational Uncertainties

A number of uncertainty contributors must be considered when addressing the accuracy of the Palisades transport calculations. These include nuclear data, reactor geometry, material compositions, definition of the neutron source distribution, and methods error. Uncertainty estimates for each of these contributions have been determined for the Palisades-specific case based on sensitivity studies, calculated flux attenuation rates in steel and water, allowable design uncertainties and as-built measurements of reactor components. Input on uncertainty estimates was also taken from other investigations [3],[10],[11],[24], and the results here are consistent with the estimates by these others. The uncertainty estimates in percent are tabulated in Table 2-1. All uncertainties are taken to be conservative estimates of one standard deviation of a normally distributed random error. While this assumption is routinely made in the treatment of uncertainty, it is not in reality a true assessment of the probability distribution in all cases. For example, for the case of a component dimension, the value may have a tolerance range rather than an uncertainty. It is likely that the probability is evenly distributed over this range with quality control assuring an almost zero probability of the dimension falling outside the range. Assuming that the tolerance range encompasses a $\pm 2\sigma$ band, the true distribution may be approximated by a normal distribution with standard deviation σ and centered on the nominal dimension. This is likely to be a good assumption for the evaluation of uncertainty in most cases.

By choosing sufficiently conservative values of the uncertainty, this treatment has been used in the analysis for this report to provide a reasonable bound to the final error estimate in the sense that the probability of the true result falling outside a $\pm 2\sigma$ band is small. Evidence to support the reasonableness and conservatism of this analysis can be found in the amount of dispersion of results in the data base of surveillance results presented in Reference [3].

Table 2-1

Palisades Calculational Uncertainty

Uncertainty Contributor	Uncertainty in Percent				
	Capsule	Vessel	Cavity	IR/ Capsule	IR/ Cavity
Nuclear Data					
Fission Spectrum	2	2	3	<1	2
Cross Sections	8	8	17	1	9
Geometry					
Core Centering	4	4	4	4	4
Capsule Location	1	(a)	(a)	(b)	(a)
Vessel Radius	(a)	6	6	6	<1
Vessel Thickness	(a)	(a)	10	(a)	10
Material Densities					
Water	4	4	4	<1	<1
Steel	1	1	4	<1	3
Source Dist.	8	8	8	5	5
Methods Error	4	4	7	2	5
Total	13	15	24	9	16

(a) Zero or Negligible Contribution
(b) Included in Experimental Uncertainty

In assessing the uncertainties, it is assumed that each uncertainty contributor can be regarded as independent (except where noted), and the uncertainties are small enough that they can be treated individually using perturbation theory. The assumption that the uncertainties are independent is true for most of the different parameters, but unknown correlations can exist. For example, a larger vessel radius could be correlated with a thinner vessel due to machining of the inner radius to round the vessel. This would result in these variations partially compensating for each other. The use of perturbation theory is supported by the small size of the flux changes (cf. Table 2-1) with the allowable changes in parameters and by the sensitivity studies in Reference [3].

The total uncertainty is calculated from the individual parts by summing in quadrature (i.e. the total variance is the sum of the variances of each factor). The uncertainties in Table 2-1 were estimated for the calculated flux at the capsule location, the vessel inner radius (IR), and the cavity. In addition, the uncertainty on the ratio of vessel IR flux to the capsule flux and to the cavity flux were calculated. These uncertainties on the flux ratios take account of the correlation of much of the uncertainty between the locations. For example, both the capsule and vessel flux will be equally affected by the neutron transport uncertainty through the core barrel and downcomer water.

Nuclear Data Uncertainties

Nuclear data uncertainties that contribute to uncertainty in calculated flux are present in the fission spectrum shape and in the cross sections for each material in the reactor geometry. The fission spectrum has only a relatively small impact on the flux ($E > 1$ MeV) because it is well known in the few MeV region. Some additional uncertainty is introduced from the fuel burnup dependence (shift of fissions from U-235 to Pu-239 and other isotopes). The uncertainty contribution will be larger for higher energy neutrons, as measured by the copper reaction for example. Uncertainties in the number of neutrons per fission and the energy per fission could also be considered as nuclear data uncertainties, but have been included below as part of the uncertainty in source normalization.

Cross section uncertainties are included for all elements, but the biggest contributor comes from the uncertainty in neutron transport through steel. Since Palisades does not have a thermal shield, a lower uncertainty estimate than for most other plants is obtained for points at the inside of the vessel. Based on Reference [11], the steel cross section, and in particular the iron inelastic cross section uncertainty, is usually considered to be the largest contributor to bias in calculated cavity flux levels of all the nuclear data uncertainties. Quantitative estimates of the cross section contributions to the flux uncertainty are given in Table 2-1 based on Maerker's LEPRICON studies reported in

this reference. It should be noted that since the studies necessary to identify the exact contributors to bias in the flux calculations have not been completed, as discussed in Section 1, the cross section uncertainties are used here to contribute to uncertainty in the flux and not as a bias in the calculated flux. The correlations in the calculations due to the fact that the cross section uncertainties result in consistent biases in the calculated fluxes have been taken into account in the estimates for uncertainty for extrapolating the experimental measurements (cf. also the discussion in Section 5 on ENDF/B-IV vs ENDF/B-VI cross sections).

Uncertainties in Geometry and Materials

Geometry uncertainties are another major contributor to uncertainty. Included for Palisades are considerations in the centering of the core relative to the vessel wall, location of the surveillance capsule, the vessel radius, and the vessel thickness. Other small uncertainties are introduced by the inclusion or exclusion of structures such as former plates that introduce non-uniformity in the axial dimension or surveillance capsules that are not present in all octants. Based on the uncertainty assessment as summarized in Table 2-1, the two most important contributors to the uncertainty are the vessel radius (for fluence calculation of the vessel and relation to the surveillance capsule) and the vessel thickness (for the relation between cavity dosimetry and the vessel fluence).

The uncertainties in flux that come from each geometry uncertainty and material density uncertainty were evaluated from the Palisades neutron transport calculation using the flux slopes in the water and steel regions to determine sensitivities. It was found that the flux decreased by 12% per cm in the water and 15% per cm in the steel. Small changes in water or steel amounts were then calculated to have an effect proportional to these flux slopes. The values derived in this way were found to be completely consistent with the sensitivity study results reported in Reference [3].

The vessel radius (inside of the stainless steel cladding) was specified on the drawings to be a minimum of 86 inches (218.44 cm). The minimum radius of the clad-base metal interface is then 86.25 inches (219.075 cm). On the shop traveler forms, the vessel base metal was found to fall between 218.90 cm and 219.74 cm (before addition of the cladding). It may be assumed that after machining, the vessel would meet the minimum radius criterion. The calculation used the 218.44 cladding radius which then gives the maximum fluence. It is conservatively assumed that the 0.84 cm range of the measured radius can be taken to be a $\pm$0.42 cm standard deviation. The effect of this radius uncertainty is a 6% uncertainty on the fluence at the vessel IR (this is treated here as an uncertainty rather than a bias, but the answer has been biased in a conservative direction by considering the minimum radius).

In addition to the radius uncertainty, an uncertainty is included due to possible variation in centering of the core relative to the vessel. An upper limit uncertainty for this effect (4%) was assigned based on the cavity dosimetry results from measurements in different quadrants [15]. By defining the uncertainty in this way, it also includes any deviation of the core power distribution from the octant symmetry assumed in the calculation. This uncertainty is larger than would be assigned on the basis of typical reactor tolerances [3].

The vessel thickness was assumed to be 8.5 inches in the calculation. The best data available from the shop traveler indicates a thickness of 8.75 $\pm$0.25 inches. The 0.25" thickness bias gives a 10% bias in the calculated result and the $\pm$0.25" indicates an uncertainty of 10%. This bias and uncertainty was not previously considered in assessing the cavity dosimetry impact on evaluation of the vessel fluence, since these are larger than the generic values indicated in [3] and [11].

The capsule dosimetry location uncertainty and the cavity dosimetry location uncertainty are discussed in Section 3. Because of the small tolerance on capsule positioning, the contribution to the calculated flux uncertainty in the capsule is estimated to be only 1%. Uncertainty on dosimetry positioning is also included in the measurement uncertainty analysis. There is also an uncertainty in the surveillance capsule calculated flux perturbation is present due to the approximations inherent in the calculational model of this structure. The magnitude of the capsule flux perturbation is about 8% and therefore a conservative 1σ estimate of the uncertainty in this perturbation is 2%. This has been included in the modeling uncertainty.

Table 2-1 also includes an uncertainty contribution from density of the water and of the steel. The water density depends on temperature and an estimated 1σ temperature variation of 5° F was used to derive the uncertainty of 4% on fluence. This value is, of course, higher per unit temperature variation due to the greater distance of water with the thermal shield absent. Similar estimates were made for an estimated steel density variation of 1%. The steel variation may also be taken to include the small tolerance on thickness of the shroud and barrel, since the effect of these is small. (Increase in steel thickness results in a decrease in water thickness, and, using the sensitivities given above, results in only a 15% - 12% or 3% change per cm.)

Other Uncertainties

The uncertainty contribution from the neutron source was evaluated considering source normalization (including neutrons per fission and energy per fission), burnup effects, radial source distribution, assembly power accuracy, and axial source distribution. Together these were estimated to contribute a total uncertainty of 8% based on the estimated uncertainty in each contributor from reference [3] as applied to Palisades. The

partial uncertainties in this total are 4% for axial shape, 5% for the relative outer assembly power, 5% for burnup effects on source distribution and normalization (including neutrons produced per unit power), and 2% for overall power normalization. Some of these terms do not contribute when relative flux is considered but the main uncertainty contributor to the vessel fluence relative to the surveillance capsule is the relative azimuthal and axial shape. These are estimated to total 5% for this relative flux. For the cavity, due to the number of measurement points, the details of the azimuthal shape are less important, but the uncertainty has been left at 5% for this case also because of the possible change in azimuthal shape between the vessel IR and the cavity (see also the discussion of neutron streaming in the cavity in Section 3.4). This uncertainty can possibly be reduced by carrying out an R-Z calculation to check these effects.

Other uncertainties in the calculation due to the modeling and transport calculation limitations are included in Table 2-1 as methods error. The reactor model used has a finite number of points that have to represent geometry in a symmetry not always appropriate. In the case of typical two dimensional calculations of LWR geometries, the fuel and shroud region is in an x-y configuration while the other reactor components in the calculation (barrel, water gap, reactor vessel, etc.) are cylindrically symmetric. Errors due to such modeling difficulties were minimized by use of a sufficient number of points to define the geometry and by paying close attention to preserving the volume of each component in the model.

The fine mesh spacing used in the calculations ensured that the neutron flux changes between mesh were sufficiently small that the calculation converged to an accurate solution. In particular, changes in the neutron flux above 1 MeV between mesh in the surveillance capsule and surroundings were held to about 10% and in the reactor vessel to less than about 20%. Experience with S_n calculations indicates that these mesh-to-mesh variations are well below allowable levels for attainment of reliable results.

Based on the estimated uncertainties due to these modeling limitations and quadrature limitations, an uncertainty estimate of about 3-4% inside the vessel was found based on experience and the sensitivity studies described in [3] and [11]. The estimate at the vessel surface is slightly higher than for the capsule due to higher uncertainty at the vessel peak fluence point. The capsule includes a contribution for uncertainty due to the capsule perturbation. In the cavity, the methods error is higher due to cavity streaming. The derivation of the magnitude of this effect is discussed in Section 3.4.

Total Uncertainty

Examination of the total uncertainties indicates that the calculation of the vessel IR fluence has an expected uncertainty of 15%. Values of fluence derived from the measurements at the capsule will have an uncertainty of 9% which must be added in quadrature to the capsule measurement uncertainty. Similarly, the cavity measurements will have an additional uncertainty of 16% added in quadrature to the cavity measurement uncertainty when extrapolating to the vessel IR. This latter estimate is larger than was used in the earlier uncertainty estimates [25] due to the increased uncertainty in vessel thickness.

3. Measurements

This section discusses uncertainties in measured data and the derivation of fluence from the measured data. Then the available Palisades plant-specific measurement data and uncertainties in that data that relate to the determination of the reactor vessel fluence are evaluated. These data consist of an in-vessel wall capsule located at 290° (W-290) which was irradiated during Cycles 1 to 5, and cavity dosimetry data from monitors irradiated during Cycle 8. Additional data from cavity dosimetry and a replacement W-290 capsule irradiated during Cycle 9 are currently being analyzed but are not available as this report is written.

An additional capsule irradiated in an accelerated position has also been analyzed [26], but these data have not been included in the vessel fluence evaluation since the location is farther from the vessel and leads to a greater uncertainty in extrapolation. The measured data also suffer from the lack of an analysis of the U-238 monitor which was recovered as powder. (The U-238 monitor has the best response of the available dosimeters in the capsule to determine flux greater than 1.0 MeV and also gives the best time integration.) Reference [26] gives the capsule fluence as 4.4 E19 n/cm^2 which is concluded to be below the calculated value and falls well below an estimated value of 6.0 E19 n/cm^2 extrapolated based on the present calculation of the Cycle 1-5 average flux with no accelerated capsule present. The measurement result was reevaluated by Simons [27] who obtained a result of 6.06 E19 n/cm^2 or an increase of 38%. Simons, however, used an inaccurate power history to evaluate the reaction rates and did not have an appropriate spectrum for the Palisades A-240 location available for his analysis. Therefore, Simons' result is not recommended.

3.1 Generic Measurement Accuracy

In general radiometric measurements can be made to an accuracy in the range of 2-5%. This accuracy has been established through calibrations of the Westinghouse laboratory with standards from the National Institute of Standards and Technology (NIST), through round-robin testing with other laboratories, and through experience with consistency of similar measurements . Maintaining high accuracy measurements is a continuing process that is followed rigorously to produce the consistency proven by the large base of data now available.

The consistency of measurements from several radiochemistry laboratories was checked by the PSF Interlaboratory Intercomparison [13]. This study concluded that there were some calibration problems in one lab that led to 40% biases, but the other labs, including Westinghouse, produced results that fell within $\pm$5% for non-fissile dosimeters and

within $\pm$10% for fission dosimeters. These results are not inconsistent with the uncertainties assigned for the Palisades analyses.

As noted above, in the discussion on Palisades capsule A-240, the analyses of fluence in the earlier years of the nuclear power industry may be suspected to have biases substantially larger than 10%. In the capsules that were reanalyzed by Simons, changes in fluence evaluations averaged 25% [27]. This magnitude of error has been greatly reduced as a result of improvements from the LWR-PV-SDIP efforts, improvements in cross-section validation, and improvements in calculational methodology. As was stated by Serpan in 1987 [28]:

> "For more than a decade, researchers of many countries have worked tirelessly to develop and perfect analysis and measurement methods of neutron dosimetry....The NRC certainly is pleased with the results; we use the improved, accurate dosimetry results extensively as the basis upon which we gain assurance of the accuracy and reliability of the submittals involving neutron flux and fluence."

3.2 Derivation of Fluence from Measurements

Values of key fast neutron exposure parameters can be derived from the measured reaction rates using the calculated spectral average cross sections for each reaction. For example, the flux (E > 1 MeV) is given by the ratio of the measured reaction rate to the calculated reaction rate over the calculated flux (E > 1 MeV). An average of the flux determined from all of the dosimeters then provides a good determination of the flux as long as the calculated spectral shape is close to the actual spectrum. This assumption can be tested by the agreement between the flux values as determined by the various threshold monitors which respond to different neutron energies. This method of flux determination does not provide uncertainty estimates that take into account the degree to which each dosimeter responds to the total flux above 1 MeV. Thus, deviations of the calculated neutron spectrum from the actual spectrum seen by the dosimeters are not taken into account. In most cases, if the calculated spectrum is derived using the methods described in Section 2, it is good enough to give an answer within the standard deviation of the measured points, as is demonstrated by comparison with the result from the least squares adjustment method to be described next.

An alternative method for derivation of fast neutron exposure from the measured data and calculated spectrum is to use a least squares approach. A code that has been extensively applied for this purpose is the FERRET least squares adjustment code [29]. The FERRET approach uses the measured reaction rate data and the calculated neutron energy spectrum at the sensor set location (surveillance capsule or cavity dosimetry set

center point) as input and proceeds to adjust the *a priori* group fluxes (trial spectrum) to produce a best fit (in a least squares sense) to the reaction rate data. The exposure parameters along with their associated uncertainties are then obtained from the adjusted spectrum.

In the FERRET evaluation, a log-normal least-squares algorithm weights both the *a priori* values and the measured data in accordance with the assigned uncertainties and correlations. In general, the measured values f are linearly related to the flux ϕ by by some response matrix A:

$$f_i^{(s,\alpha)} = \sum_g A_{ig}^{(s)} \phi_g^{(\alpha)}$$

where:

i indexes the measured values belonging to a single data set s,
g designates the energy group, and
α delineates spectra that may be simultaneously adjusted.

For example,

$$R_i = \sum_g \sigma_{ig} \phi_g$$

relates a set of measured reaction rates R_i to a single spectrum ϕ_g by the multigroup cross-section σ_{ig}. (In this case, FERRET also adjusts the cross-sections.) The log-normal approach automatically accounts for the physical constraint of positive fluxes, even with large assigned uncertainties.

In the FERRET analysis of the dosimetry data, the continuous quantities (i.e., fluxes and cross-sections) are approximated in 53 energy groups. The calculated fluxes (*a priori* input) are expanded into the FERRET group structure using the SAND-II code [30]. This procedure is carried out by first expanding the *a priori* spectrum into the SAND-II 620 energy group structure using a SPLINE interpolation procedure for interpolation in regions where group boundaries do not coincide. The 620 group spectrum is then easily collapsed to the group structure used in FERRET.

The cross-sections were also collapsed into the 53 energy group structure using SAND-II with the calculated spectrum (as expanded to 620 groups) as weighing function. The cross sections were taken from the ENDF-B/V dosimetry file. Uncertainty estimates in the form of 53 x 53 covariance matrices have been constructed for each cross-section

based on the ENDF-B/V files. Correlations between cross-sections for different reactions are neglected due to data and code limitations, but this omission does not significantly impact the results of the adjustment.

For each set of data or *a priori* values, the inverse of the corresponding relative covariance matrix M is used as a statistical weight. In some cases, as for the cross-sections, a multigroup covariance matrix is used. More often, a simple parameterized form is employed:

$$M_{gg'} = c_n^2 + r_g \, r_{g'} \, \rho_{gg'}$$

where c_n specifies an overall fractional normalization uncertainty (i.e., complete correlation) for the corresponding set of values. The fractional uncertainties r_g specify additional random uncertainties for group g that are correlated with a correlation matrix:

$$\rho_{gg'} = (1-\theta) \, \delta_{gg'} + \theta \, \exp -[\frac{(g-g')^2}{2\gamma^2}]$$

The first term specifies purely random uncertainties while the second term describes short-range correlations over a range γ (Θ specifies the strength of the latter term). The value of δ is 1 when g equals g' and 0 otherwise.

For the *a priori* calculated fluxes, a short-range correlation of $\gamma = 6$ groups was used. This choice implies that neighboring groups are strongly correlated when Θ is close to 1. Strong short-range correlations (or anticorrelations) were justified based on information presented by R.E. Maerker [31]. Maerker's results are closely duplicated when $\gamma = 6$. For the integral reaction rate covariances, simple normalization and random uncertainties were combined as deduced from experimental uncertainties.

In performing least squares adjustments with the FERRET code, the neutron flux spectrum calculated at the center of the dosimetry location is input to the analysis. Typical uncertainties in the input (*a priori*) spectra and the measured reaction rates used in the FERRET evaluations are as follows:

Flux Normalization Uncertainty (c_n)	30 percent
Flux Group Uncertainties (r_g)	
(E > 0.0055 MeV)	30 percent
(0.68 eV < E < 0.0055 MeV)	58 percent
(E < 0.68 eV)	104 percent
Short-Range Correlation Strength (θ)	
(E > 0.0055 MeV)	0.9
(0.68 eV < E < 0.0055 MeV)	0.5
(E < 0.68 eV)	0.5
Flux Group Correlation Range (γ)	
(E > 0.0055 MeV)	6
(0.68 eV < E < 0.0055 MeV)	3
(E < 0.68 eV)	2
Reaction Rate Uncertainty	5-10 percent

The reaction rate uncertainty estimates include both a statistical (counting) uncertainty and systematic uncertainty. The latter is based on known errors such as uncertainty in counter efficiency, unknown errors that are derived from consistency of counting results, and estimates of error arising from the power history and corrections for competing reactions. Specific discussion of these uncertainty contributors may be found in Section 3.3.

It should be noted that the uncertainty listed for the upper energy range extends down to the lower ranges. Thus, the 58 percent group uncertainty estimate for each group in the second range is made up of a 30 percent uncertainty with a 0.9 short-range correlation and a range of 6, and a second part of magnitude 50 percent with a 0.5 correlation and a range of 3 that represents additional uncertainty on the spectrum shape in the resonance region. (Of course for problems with threshold reaction rate measurements, the resonance region analysis does not affect the high energy neutron flux result.) These input uncertainty assignments were based on prior experience in using the FERRET least squares adjustment approach in the analysis of neutron dosimetry from surveillance capsule, reactor cavity, and benchmark irradiations. The values are liberal enough to permit adjustment of the input spectrum to fit the measured data for all practical applications.

For the Palisades evaluation, both the averaging and the FERRET method have been applied. However, the recommended results are based on the FERRET analysis because the results from FERRET are conservative relative to the averaging method and because the FERRET method better utilizes the total information available about the problem to define the flux and uncertainty.

3.3 Palisades Capsule Measurement and Uncertainty

Measured reaction rates for the Palisades W-290 surveillance capsule are given in the capsule report [17], and are summarized in Table 3-1. In this table, an average value is calculated based on the middle and top measurement positions only. This results in a slightly higher average measured activity since the bottom position measurements are all biased low. This result is in slight disagreement with the calculated axial power shape and this is taken into account in the uncertainty assignments.

Table 3-1

Capsule W-290 Measured Activities

	Measured Activity (Bq/g)			
Reaction	Top	Middle	Bottom	Average[a]
Cu63(n,α)Co60	2.32E+05	2.39E+05	2.07E+05	2.36E+05
Fe54(n,p)Mn54	1.85E+06[b]	1.82E+06[b]	1.58E+06[b]	1.84E+06
Ni58(n,p)Co58	3.06E+06	3.05E+06	2.90E+06	3.06E+06
U238(n,f)Cs137	5.56E+05		5.36E+05	5.56E+05
Ti46(n,p)Sc46	1.10E+05	1.06E+05	1.01E+05	1.08E+05

(a) Average of top and middle measurements

(b) Fe measurements are average of 6 values at each location

Table 3-2 gives the derived reaction rates based on the average activities. In this table, a correction factor is listed. This factor is a correction for the changing ratio of the flux/power at the capsule compared to the average for the 5 cycle irradiation. These factors are derived for each monitor based on the relative flux values for each cycle as

tabulated in Table 3-3. Since this flux variation was not previously accounted for, these corrections represent a change to the capsule report values. Another change was the updating of the U-238 fission yield for cesium to the currently used value of 5.99%.

Table 3-2

Capsule W-290 Reaction Rates

Reaction	Activity[a]	Correction	Saturated Activity[a]	Reactions /s/atom
Cu63(n,α)Co60	2.36E+05	0.98	6.84E+05	1.044E-16
Fe54(n,p)Mn54	1.84E+06	0.94	5.31E+06	8.490E-15
Ni58(n,p)Co58	3.06E+06	0.94	7.27E+07	1.038E-14
U238(n,f)Cs137	5.56E+05	1.00	4.68E+06[b]	3.090E-14
Ti46(n,p)Sc46	1.08E+05	0.94	1.65E+06	1.620E-15

(a) Units of activity are Bq/g.
(b) Corrected for U-235 and Pu-239 fission contributions.

Table 3-3

Power History for W-290 Capsule

Cycle	Length (EFPY)	Relative Flux
1	1.039	0.959
2	1.230	0.850
3	0.958	1.065
4	0.898	1.111
5	1.081	1.061

A summary of the uncertainty components and total uncertainty in each reaction rate are given in Table 3-4. The uncertainty contributors include random error in the measurement, systematic error in the measurement, and uncertainty in the derivation of reaction rates from the measured decay rates. Each of these components will be briefly

addressed below. Another uncertainty, that of dosimeter position, is not included in the error in reaction rates and this uncertainty will be discussed in the context of comparison of the measurements with the calculation.

Table 3-4

Uncertainties in W-290 Reaction Rates

	Estimated Uncertainty (%)			
Reaction	Random	Systematic	History	Total
Cu63(n,α)Co60	4	3	1	5
Fe54(n,p)Mn54	2	3	3	5
Ni58(n,p)Co58	4	3	6	8
U238(n,f)Cs137	9	4	<1	10
Ti46(n,p)Sc46	4	3	6	8

Measurement Uncertainty

The measurement of the radioactive decay of each dosimeter is carried out by placing the dosimeter in a calibrated position relative to a germanium detector and measuring the number of gamma rays recorded by the detector per unit time that deposit their full energy in the detector. After subtracting background, the detector calibration curve (together with the gamma yield per decay for the isotope in question) is used to determine the number of decays per second (dps) in the dosimeter. After determining the amount of target material in the dosimeter and correcting for any impurity response, the dps per target atom is then calculated. Uncertainty in the measured dosimeter response will be made up of a set of random uncertainties and systematic error. The random uncertainty consists of contributions from the statistical error in the number of counts (including a contribution for the background subtraction), uncertainty in the determination of the mass of dosimeter material, and uncertainty in the sample positioning for counting. Typical values assigned by the radiochemistry laboratory for this uncertainty are 1-3%, but consistency of data sets indicates that a more conservative value of 4-5% should be used (cf values given in Reference [3]).

Specific uncertainty values for the Palisades measurements are given in Table 3-4. In this table conservative estimates for the random error are given for each reaction. These are each 4% except for the iron reaction which consisted of 6 measurements at each of the three locations, and the U-238 fission reaction which has a larger uncertainty due to corrections for fission in U-235 impurity, fission in Pu-239 that builds in during the irradiation, and photofission. The U-238 reaction also had fewer measurement results.

The systematic error arises from the detector calibration error, nuclear data errors (gamma yield, fission yield), isotopic abundance uncertainty, and other consistent measurement bias. All these errors are minimized by consistent calibration to standards, round-robin testing, and benchmark referencing. Table 3-4 includes an estimate of the systematic error and also a contribution due to flux history uncertainty at the dosimetry position to be discussed next. The uncertainty assessment here is broken down in a different way than the generic assessment of measurement uncertainty in Reference [3], but the total uncertainty for each reaction is quite close with the assessment for Palisades being slightly more conservative. In the reference analysis, the counting uncertainty includes the random and calibration error, the decay correction uncertainty includes the flux history and nuclear data uncertainty, and the competing fission reaction uncertainty is handled separately.

Reaction Rate Uncertainty

The derivation of the reaction rate (i.e. reactions per second per target nucleus in the dosimeter at full reactor power) from a measured decay rate depends on the time-history of the irradiation. Usually the reactor power-history is used for this evaluation. Since the dosimeter reactions depend on the actual neutron flux at the dosimeter location, error is introduced since this flux will not be exactly proportional to the reactor power. Deviations in relative flux are caused by changes in reactor power distributions and fuel burnup effects, and also may be affected by changes that occur in water temperature or other reactor parameters. Uncertainties in half-lives of the produced radioactive isotopes and in the reactor power history can also contribute, but in most cases (including the Palisades data), these uncertainties are much smaller than the uncertainty in the changing flux/power ratio and can be neglected. The changes with burnup can affect both the relative flux level and the neutron spectrum, but the spectrum changes are second order and also can be neglected.

In the case of the Palisades W-290 capsule, irradiation extended over 5 fuel cycles. Thus both errors in relative dosimeter activation rate between cycles and during the cycle duration need to be addressed. Bias and error due to the changing flux to power ratio were not addressed in the previous analyses [17],[25]. The details of the cycle power

generation and the relative flux at the capsule location are given in Table 3-3. The impact of the history uncertainty on each reaction rate is tabulated in Table 3-4.

During a fuel cycle, the change in core power distribution with fuel burnup will change the relative neutron leakage. The change in leakage can be broken into two parts. First, due to a higher burnup rate in the higher power fuel assemblies in the middle of the core, the power generated by the outer fuel assemblies generally increases with core age. This effect is minimal, however, when fresh fuel is placed on the periphery as was the case in Palisades for the time when capsule W-290 was irradiated. The second part of the leakage change is caused by a reduction in power in the axial region of highest power generation and an increase at the top and bottom of the core to compensate. Figure 3-1 illustrates the difference between the axial power shape for Cycle 5 calculated for the end-of-cycle (EOC) compared with the average axial shape. The average shape is used for the calculation and thus the average is a proper basis for comparison to estimate deviations seen by the dosimeters.

Figure 3-1

Palisades Cycle 5 Axial Power Shapes

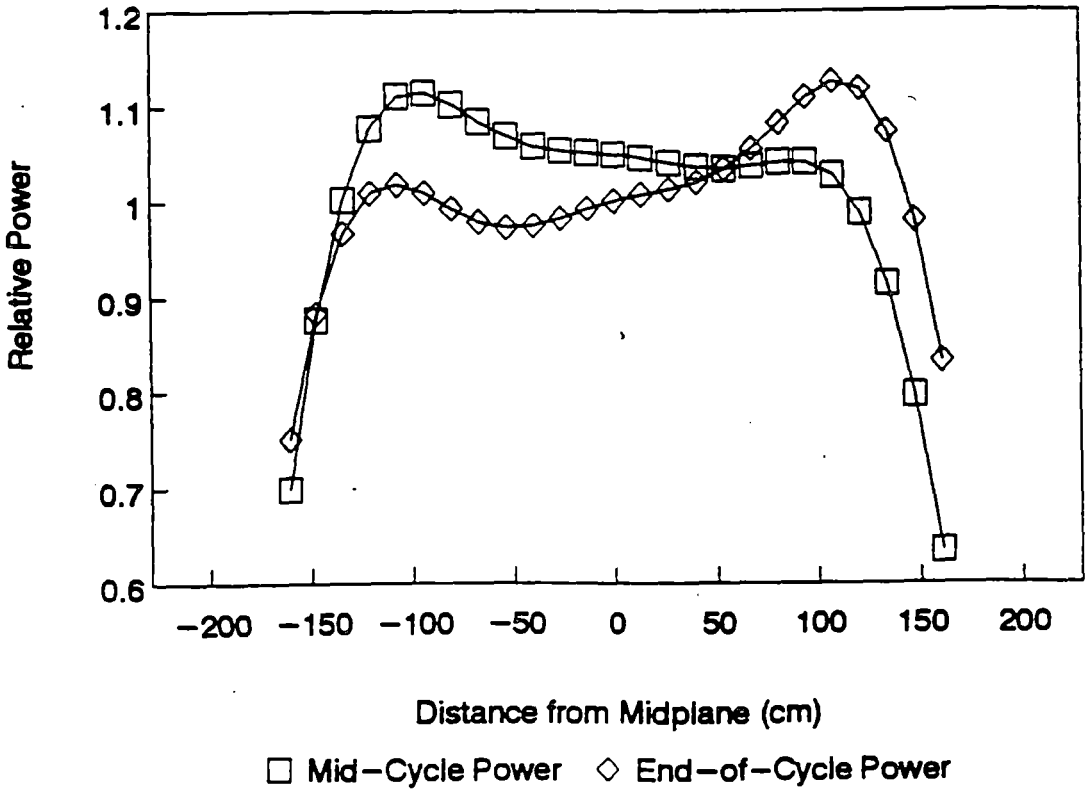

For evaluating the effect of the axial shape change during the cycle on reaction rate measurements, only the shorter-lived radioactive products need to be considered. These are the Ni(n,p) and Ti(n,p) reactions. Because these reactions only respond to the last irradiation cycle, only the Cycle 5 axial shape changes are important. The longer-lived monitors provide a better integral over the irradiation time and thus provide an average response that is almost independent of such changes. Calculations indicate that for Cycle 5, which has fresh fuel on the periphery, the increase in edge assembly power near the W-290 capsule is about 4% during the cycle. In contrast, the decrease in power in the region near midplane is also about 4%. Thus, the indicated correction to the nickel and titanium monitors for the net change in peripheral power is nil for dosimetry located near axial midplane region where axial power gradients are small. The correction is not negligible, however, for locations nearer the top or bottom edge of the core where the axial shape changes are more pronounced. This can be observed in the data (Table 3-1) by comparing the midplane and bottom Ti and Ni (ratio of 1.05) with the Cu and Fe (ratio of 1.15), indicating that the bottom short-lived dosimeters are responding to an increase in the flux level at the end of the fuel cycle while the Cu and Fe are averaging over the entire cycle.

In the previous analysis, average values were used for the capsule to minimize stochastic variation in the data. This averaging ignores axial flux gradients in the capsule, which the data indicates are as large as 15%. Thus the average of the three locations could be biased below the maximum reaction rate value by about 15/3 or 5%. This has been eliminated in this analysis by using the average of the top and middle reaction rates and not using the lower bottom measurements in the average. There still remains an uncertainty in whether the two points are at the maximum flux, even though the calculated average axial shape is almost flat in the center region. This is included as an additional uncertainty added to the position uncertainty discussed below, to account for this possible deviation of the measurements from the maximum axial point. Since this is included in the position uncertainty which affects the C/M ratio but not the uncertainty in the measurement itself, this contribution is not included in Table 3-4.

Dosimetry Positioning Uncertainty

The reactor drawings specify an uncertainty on the radial location of the surveillance capsule of 1/16 inch. This will contribute an uncertainty of only 1% to the flux. The azimuthal uncertainty in capsule location is 0.5° which contributes an additional 1% uncertainty. These uncertainties are included in Table 2-1 as a contributor to the calculated capsule flux uncertainty but have been added here to the dosimeter positioning uncertainty for the total experimental uncertainty. There is also an uncertainty in the position of the dosimeters within the capsule. This is specified as 1/32 inch which introduces a flux uncertainty of less than 1%. As mentioned above, there is also an axial

uncertainty that arises from difference between the axial measurement locations and the axial flux peak due to the uncertainty in the calculated flux shape. This uncertainty is conservatively estimated at 5% based on Figure 3-1.

Combining the above uncertainty estimates gives a total of 5%. This must be added to the measurement error to give a total uncertainty in the C/M value.

Capsule Fluence Derivation

The updated reaction rates (Table 3-2) and uncertainty estimates (Table 3-4) were input to the FERRET code and an adjusted spectrum was derived. The calculated (*a priori*) spectrum and the adjusted spectrum are given in Table 3-5. This table also indicates the uncertainties for the flux in each energy group. Although these uncertainties are fairly large, when integral results are calculated the uncertainty correlations result in a greatly reduced uncertainty. The FERRET result for the flux (E > 1 MeV) at the surveillance capsule center is 6.71 E10 n/cm^2-sec which is slightly below the value in the original capsule report (6.95 E10 n/cm^2-sec). The uncertainty in FERRET least squares fit value is 9%. The quality of the derived value is supported by the excellent agreement of the reaction rates calculated with the adjusted flux-spectrum with the measurements as shown in Table 3-6. Compared with the calculated value for the average flux in the W-290 capsule (7.36 E10 n/cm^2-sec), the FERRET value falls low by 9% (C/M is 1.10).

A comparison of the calculated and measured reaction rates was also made. This appears in Table 3-6 in the column Calc/Meas for the *a priori* spectrum. These values all indicate that the calculation is higher than the measured values. This comparison differs from that in the original capsule report in that the ENDF-B/V dosimetry cross sections are used and these are collapsed using the spectrum calculated for this study. The new calculation has a better geometrical representation and thus is expected to provide an improved spectral shape. An assessment of the uncertainty of the comparison of measured reaction rates and calculation is given in Table 3-7. In this table the uncertainties due to measurement (Table 3-4) are given in the second column, dosimetry positioning (discussed above) in the fourth column, and dosimeter cross sections in the third column. The latter uncertainties are the uncertainties in the capsule spectral average cross sections for each reaction. These were calculated by the FERRET code using the ENDF/B-V cross section uncertainty correlation matrix. Table 3-7 also presents the C/M ratio for each reaction and its associated uncertainty derived by combining in quadrature the three components in the table.

As indicated in Table 3-7, the direct comparison of the reaction rates with calculation indicates that the calculation is high by 15%. This value has an uncertainty of 7% as derived from the weighted statistical average of the measurements combined with the

Table 3-5

FERRET Least Squares Adjustment Results
Palisades Capsule W-290

Group	Energy (MEV)	A Priori Flux* ($n/cm^2/sec$)	Adjusted Flux ($n/cm^2/sec$)	Percent Uncert. (1 STD)
1	17.33	1.105E+07	9.557E+06	23
2	14.92	2.665E+07	2.281E+07	20
3	13.50	1.186E+08	1.007E+08	18
4	11.62	2.969E+08	2.507E+08	15
5	10.00	7.098E+08	5.983E+08	12
6	8.607	1.274E+09	1.078E+09	11
7	7.408	3.221E+09	2.741E+09	10
8	6.065	4.612E+09	3.964E+09	10
9	4.966	8.119E+09	7.075E+09	9
10	3.679	7.695E+09	6.851E+09	11
11	2.865	1.234E+10	1.125E+10	12
12	2.231	1.133E+10	1.056E+10	14
13	1.738	1.126E+10	1.065E+10	17
14	1.353	8.519E+09	8.133E+09	20
15	1.108	1.166E+10	1.125E+10	22
16	0.8208	1.054E+10	1.023E+10	25
17	0.6393	9.339E+09	9.104E+09	27
18	0.4979	6.716E+09	6.551E+09	29
19	0.3877	7.644E+09	7.443E+09	31
20	0.302	1.106E+10	1.073E+10	32
21	0.1832	9.389E+09	9.068E+09	33
22	0.1111	7.598E+09	7.303E+09	34
23	0.06738	6.305E+09	6.030E+09	35
24	0.04087	4.667E+09	4.444E+09	35
25	0.02554	3.246E+09	3.079E+09	36
26	0.01989	2.626E+09	2.483E+09	36
27	0.01503	4.702E+09	4.435E+09	36
28	9.119E-03	4.899E+09	4.613E+09	62
29	5.531E-03	5.363E+09	5.043E+09	62
30	3.355E-03	1.736E+09	1.631E+09	62
31	2.839E-03	1.680E+09	1.578E+09	62
32	2.404E-03	1.643E+09	1.543E+09	62
33	2.035E-03	4.797E+09	4.502E+09	62
34	1.234E-03	4.671E+09	4.383E+09	62

Table 3-5 continued

Group	Energy MeV	A Priori Flux* (n/cm2/sec)	Adjusted Flux (n/cm2/sec)	Percent Uncert. (1 STD)
35	7.485E-04	4.556E+09	4.275E+09	62
36	4.540E-04	4.482E+09	4.204E+09	62
37	2.754E-04	4.663E+09	4.374E+09	62
38	1.670E-04	4.738E+09	4.445E+09	62
39	1.013E-04	4.750E+09	4.455E+09	62
40	6.144E-05	4.747E+09	4.453E+09	62
41	3.727E-05	4.722E+09	4.429E+09	62
42	2.260E-05	4.678E+09	4.387E+09	62
43	1.371E-05	4.633E+09	4.345E+09	62
44	8.315E-06	4.580E+09	4.295E+09	62
45	5.043E-06	4.517E+09	4.236E+09	62
46	3.059E-06	4.433E+09	4.157E+09	62
47	1.855E-06	4.293E+09	4.026E+09	62
48	1.125E-06	4.028E+09	3.777E+09	62
49	6.826E-07	3.807E+09	3.570E+09	106
50	4.140E-07	3.957E+09	3.711E+09	106
51	2.511E-07	1.071E+10	1.004E+10	106
52	1.523E-07	1.811E+10	1.698E+10	106
53	9.237E-08	3.932E+10	3.687E+10	106

*DOT transport calculation absolute group flux converted to FERRET group structure.

positioning uncertainty. The latter is treated as correlated for all the measurements. The 7% uncertainty is larger than the standard deviation of the measurements (6%) due to the addition of this positioning uncertainty component. This uncertainty estimate does not include any uncertainty due to the uncertainty in the spectrum shape. The latter is included in FERRET which accounts for the slightly larger FERRET uncertainty. It is also noted that FERRET produces a slightly higher result. This is due to the flexibility FERRET has to adjust the spectrum which results in a higher weight to the U-238 monitor which has the largest overlap with the flux above 1.0 MeV. Within the uncertainties estimated for the calculation, and for these evaluations, the results are regarded as consistent.

Table 3-6

Comparison of Measured and Calculated Reaction Rates
Palisades Capsule W-290

Reaction	Reaction Rate (dps/nucleus)			Ratio Calc/Meas	
	Meas	A Priori Calc	Adj Calc	A Priori	Adj Calc
Cu63(n,α)Co60	1.04E-16	1.24E-16	1.05E-16	1.19	1.00
Fe54(n,p)Mn54	8.49E-15	9.78E-15	8.51E-15	1.15	1.00
Ni58(n,p)Co58	1.04E-14	1.26E-14	1.08E-14	1.21	1.04
U238(n,f)Cs137	3.09E-14	3.25E-14	2.93E-14	1.05	0.95
Ti46(n,p)Sc46	1.62E-15	1.85E-15	1.60E-15	1.14	0.99

Table 3-7

Comparison of Measurements and Calculations and
Uncertainty Assessment for Capsule W-290

	Reaction Rate Uncertainty	Cross Section Uncertainty	Position Uncertainty	C/M	Total Uncertainty
Cu63(n,α)Co60	5%	7%	5%	1.19	10%
Fe54(n,p)Mn54	5%	3%	5%	1.15	8%
Ni58(n,p)Co58	8%	6%	5%	1.21	11%
U238(n,f)Cs137	10%	3%	5%	1.05	12%
Ti46(n,p)Sc46	8%	7%	5%	1.14	12%
Average				1.15	7%

3.4 Palisades Cavity Dosimetry Measurements

Results of the Cycle 8 cavity dosimetry measurements are given in Reference [15]. Since that analysis was completed, new measurements of the dosimetry locations have been made. This established that the dosimetry sets attached to the bar were indeed shifted both radially and azimuthally. The new measurements of radial position indicate that the 16° location is shifted inward by 5.8 inches and the 26° position is shifted inward by 5.2 inches. These shifts result in increases in the calculated flux for these dosimeter sets of 11.5% and 4.5%, respectively. At the 39° position the radial shift is 3.5 inches and this gives only a very slight flux change (0.5%).

Cavity Dosimetry Positioning Uncertainty and Flux Streaming

Usually positioning error for dosimetry in the reactor cavity is not important since flux changes occur over relatively large distances at this distance from the core when no absorber is present. However, since the Palisades reactor cavity width is comparable to azimuthal distances over which flux level changes occur, streaming in the azimuthal direction can be expected. In the axial direction, the core height is much greater than the cavity width so axial streaming effects will be much smaller near midplane. There is also a small fall-off in flux with radius in the cavity due to the increase in size of the solid angle with radius. The net effect of the streaming is then a fall-off of the flux with radius in the cavity at angles with relatively higher flux (i.e. near the peak flux region at 16 degrees) and a much smaller effect at angles where the flux is at a minimum (i.e. near 0 and 45 degrees). The calculated flux fall-off with position in the cavity is shown in Figure 3-2. In this figure, the flux at each azimuthal angle has been normalized to the nominal dosimetry location. It is seen that the C/M ratio at 0 and 45 degrees will be essentially unaffected by error in radial position of the dosimetry, while a radial position error at 30 degrees has a slight effect. Around 16 degrees azimuth, however, the radial position is of greater importance and must be considered.

Another effect that will impact the C/M ratio is the accuracy of the quadrature to calculate the cavity streaming. A calculation was performed using S_{16} to compare with the standard S_8. Since the S_{16} calculation is much longer (in computer time) than the S_8, only the highest energy neutron group was calculated with the S_{16} quadrature to compare with the S_8 group one. It was found that the S_8 calculations were adequate (differences less than 2%) everywhere except in a few regions in the cavity. At the peak fluence angle (i.e. around the 16 degree azimuthal maximum) the S_{16} calculation predicts about a 5% higher group one flux at the nominal (uncorrected) dosimetry radial location. The ratio between the S_8 and S_{16} calculations is shown in Figure 3-3 for the radial location of the dosimetry.

Figure 3-2

Palisades Cavity Radial Flux Change

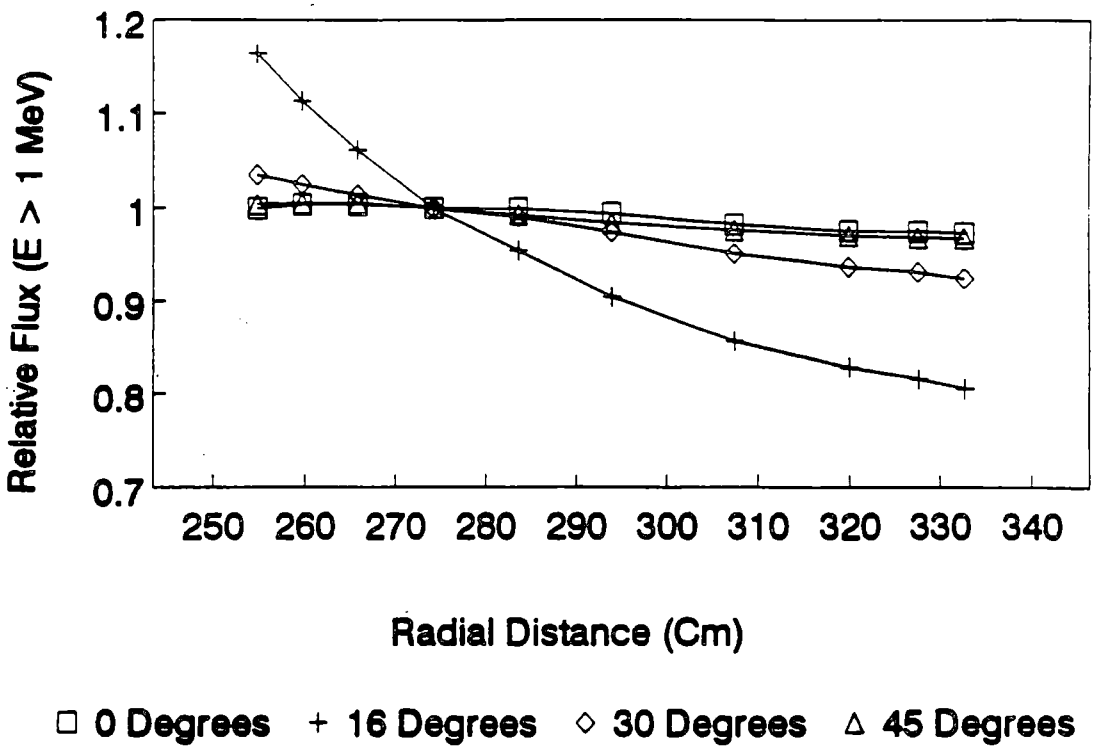

The change of flux with radius in the cavity was almost unaffected by the quadrature. This is illustrated in Figure 3-4 for azimuthal angles of 0° and 16°. Although the difference between the S_8 and S_{16} is greater at 16°, in both cases the difference between the two quadrature results changes by about 2% radially across the cavity. A comparison was also made for the S_8 calculation between group 1 (above 14.2 MeV) and the flux above 1 MeV and almost no difference in the cavity behavior was observed except that the total flux changes across the cavity were somewhat altered.

The total effect then is that the S_8 calculation is expected to be low by approximately 5% at 16 degrees and the estimated uncertainty in the C/M ratio for this particular azimuthal angle is increased by up to 5% because of the possibility of a radial position error. This provides a partial explanation for why the measurements at 16 degrees in the cavity appear inconsistent with the other data. These uncertainties do not affect the quality of the predicted fluence at the vessel inner radius near 16 degrees since these effects only

Figure 3-3

Comparison of S_8 and S_{16} in Cavity vs Azimuth

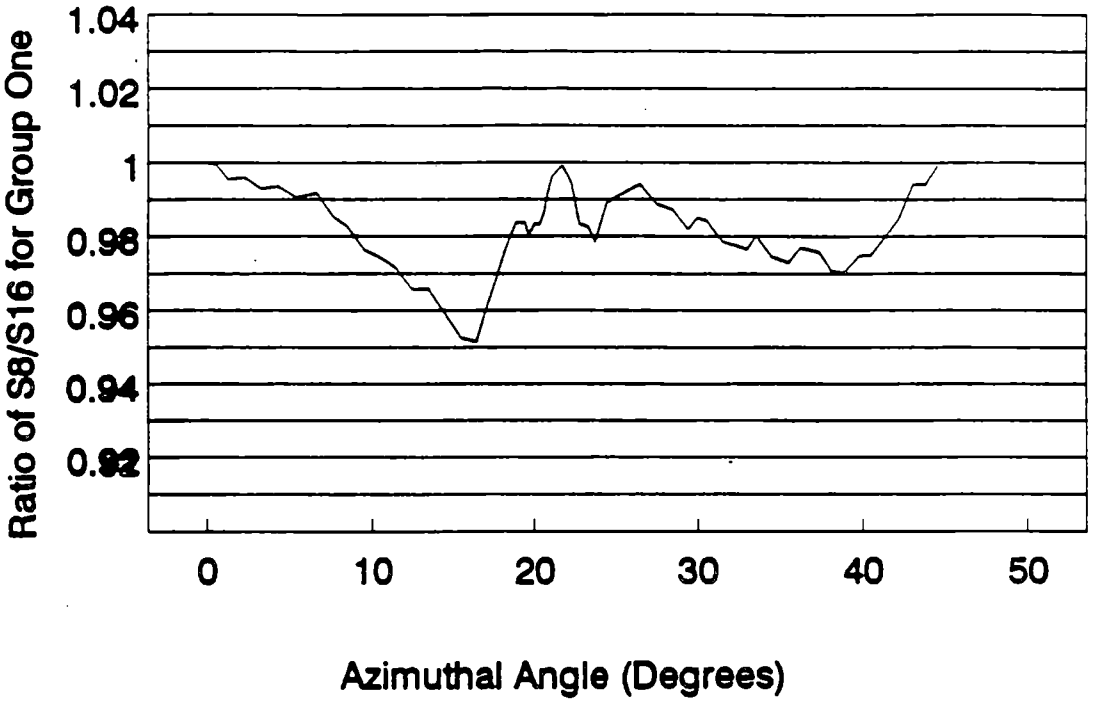

appear in the cavity and it is not recommended to use the 16 degree point by itself to extrapolate through the vessel at this angle. The 16 degree point is, however, included in the cavity average result, which provides a conservatism at the other angles. The improved quadrature result was only used to provide an uncertainty estimate rather than a bias since only the first energy group was calculated. The other fast groups are expected to behave similarily, although as the neutron energy decreases, scattering of higher energy neutrons from the back of the cavity will increase and partially ameliorate the effect.

Estimates have been made of the position uncertainty of the dosimetry sets in the cavity. These sets were all suspended from a support bar which was skewed in the cavity by a metal bar that interfered with the support chain. Measurements made of the radial bar position indicated that the dosimetry positions were shifted from nominal values and positions based on the new measurements are given in Table 3-8. This table also gives

Figure 3-4

Comparison of S_8 and S_{16} Radial Flux in Cavity

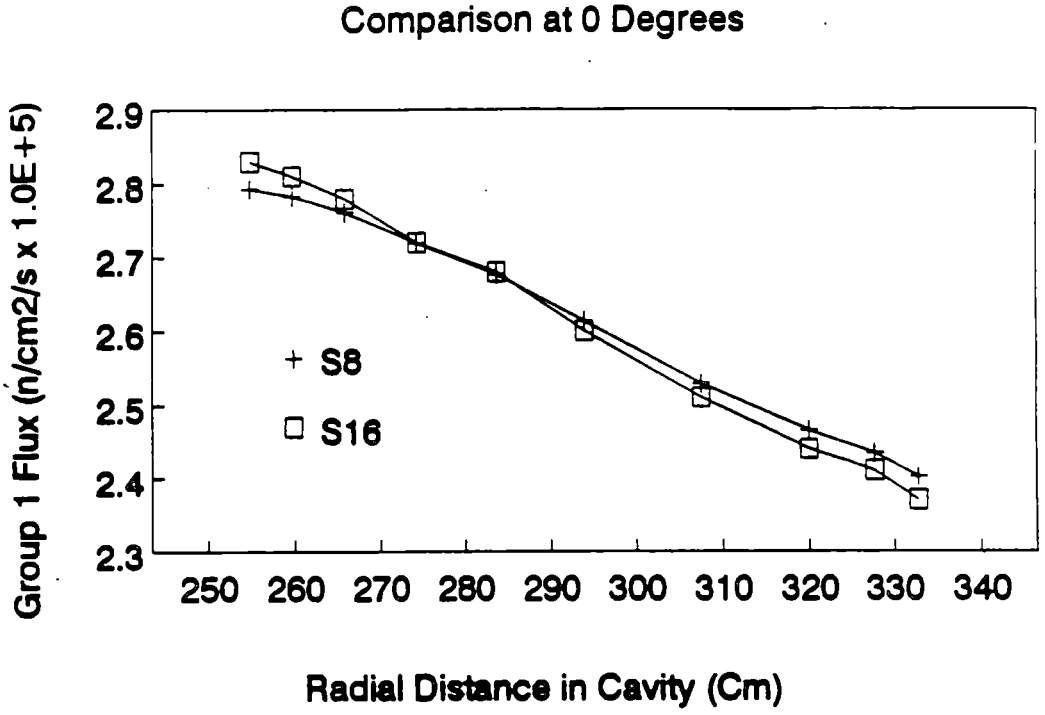

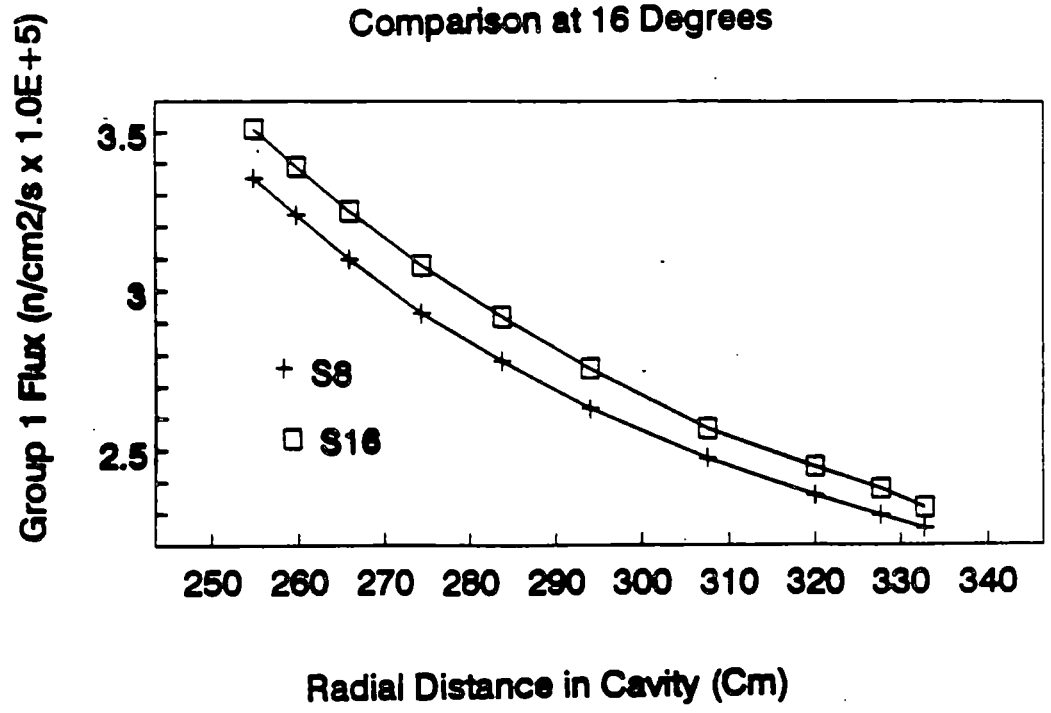

Table 3-8

Calculated Flux Uncertainties for Cavity Dosimetry

Shifted Angle	16°	26°	39°
Radial Location	259.6 cm	261.0 cm	265.4 cm
Calculated Flux (E > 1 MeV) n/cm^2-s	1.45 E+09	1.16 E+09	8.65 E+08
Flux (Nominal Dosimetry Position) n/cm^2-s	1.30 E+09	1.11 E+09	8.61 E+09
Flux Uncertainty due to 2 inch radial position uncertainty	4%	2%	<0.1%
Flux Uncertainty due to 2° azimuthal position uncertainty	2%	6%	2%
Quadrature Uncert.	5%	2%	3%
Total Position and Quadrature Uncert.	7%	7%	4%

the calculated flux at the revised position and the nominal dosimetry radial position at each angle for comparison. Uncertainties in flux due to uncertainties in these positions are taken from the calculated flux shapes in the cavity using a conservative position uncertainty assessment of ± 2 inches in the radial direction and $\pm 2°$ in the azimuthal direction. Also included in the total cavity uncertainty is the uncertainty due to the quadrature which is taken from the deviations shown in Figure 3-3. This has been included here because it is a specific uncertainty in the cavity calculation.

Another question of the cavity positioning involves the foil orientation. For the high energy reactions, orientation is not important since the cross sections are small enough that the neutron absorption in the foil is only a small fraction of the incident flux. Therefore, the foils absorb almost equally over the entire foil volume independent of the orientation. Absorption effects are also minimized since the flux is not a beam but rather distributed in angle, although forward peaked.

Measurement Results

Revised analyses are shown in Tables 3-9 and 3-10. Table 3-9 summarizes the revised FERRET results for flux (E > 1 MeV) and compares them with the transport calculation at the revised location in the cavity. The uncertainty in the C/M ratio for each dosimetry set is given. This is derived by combining the FERRET flux uncertainty of 6% at each location with the positioning uncertainty from Table 3-8. The average C/M ratio is found to be 1.06 with a standard deviation for the three measurements of 0.08. However, as noted above, a bias of 10% in the calculation is indicated due to the likelihood that the average vessel thickness is 1/4 inch greater that the nominal value. Including this bias a resultant C/M ratio of 0.96 with an uncertainty (based on the FERRET analysis and the position uncertainty) of 7%. The uncertainty in the average is not much below the individual fluence uncertainties at each angle since much of the uncertainty was assumed to be correlated (i.e. uncertainty in gamma detector calibration, spectrum shape error, quadrature uncertainty, etc.). The 7% uncertainty value is seen to be very close to the standard deviation of the three measurements.

Table 3-9

Revised Cavity Flux Comparison

Location	Measured Flux[a]	Calculated Flux[b]	C/M
16°	1.46×10^9	1.45×10^9	$0.99 \pm .07$
26°	1.10×10^9	1.16×10^9	$1.05 \pm .08$
39°	7.60×10^8	8.65×10^8	$1.14 \pm .07$
		Average C/M	$1.06 \pm .08$[c]

(a) FERRET evaluation.
(b) Flux calculated at revised dosimetry positions.
(c) Standard deviation of the three measurements.

Details of the analyses for the three midplane cavity spectral dosimetry sets are given in Table 3-10. In this table the C/M ratio for each fast reaction is given and an average calculated. Again, as for the capsule measurement, it is seen that the average C/M ratios give a lower flux than the FERRET values in Table 3-9. Use of the FERRET flux evaluation is therefore conservative.

Table 3-10

Palisades Cavity Dosimetry Results
Comparison of Measured and Calculated Sensor Reaction Rates

Reaction	Measured	A Priori Calculation	Adjusted Calculation	C/M A Priori	C/M Adjusted
		16 Degree Azimuth - Core Midplane			
Cu63(n,α)Co60	9.76E-19	1.26E-18	9.97E-19	1.29	1.02
Fe54(n,p)Mn54	7.42E-17	8.23E-17	7.46E-17	1.11	1.01
Ni58(n,p)Co58	1.04E-16	1.11E-16	1.03E-16	1.07	0.99
U238(n,f)Cs137	4.14E-16	4.34E-16	4.14E-16	1.05	1.00
Np237(n,f)Cs137	6.72E-15	6.94E-15	6.68E-15	1.03	0.99
Ti46(n,p)Sc46	1.45E-17	1.57E-17	1.42E-17	1.08	0.98
		Average C/M		1.10	1.00
		26 Degree Azimuth - Core Midplane			
Cu63(n,α)Co60	7.51E-19	1.02E-18	7.68E-19	1.35	1.02
Fe54(n,p)Mn54	5.60E-17	6.55E-17	5.65E-17	1.17	1.01
Ni58(n,p)Co58	7.81E-17	8.88E-17	7.78E-17	1.14	1.00
U238(n,f)Cs137	3.19E-16	3.48E-16	3.16E-16	1.09	0.99
Np237(n,f)Cs137	4.97E-15	5.77E-15	4.98E-15	1.16	1.00
Ti46(n,p)Sc46	1.11E-17	1.25E-17	1.09E-17	1.13	0.98
		Average C/M		1.17	1.00
		39 Degree Azimuth - Core Midplane			
Cu63(n,α)Co60	5.53E-19	7.28E-19	5.65E-19	1.32	1.02
Fe54(n,p)Mn54	4.00E-17	4.67E-17	4.00E-17	1.17	1.00
Ni58(n,p)Co58	5.51E-17	6.34E-17	5.48E-17	1.15	0.99
U238(n,f)Cs137	2.16E-16	2.52E-16	2.18E-16	1.17	1.01
Np237(n,f)Cs137	3.65E-15	4.45E-15	3.65E-15	1.22	1.00
Ti46(n,p)Sc46	7.89E-18	8.93E-18	7.74E-18	1.13	0.98
		Average C/M		1.19	1.00

Based on the analyses above, it may be concluded that the calculation alone at the vessel inner radius produces results with an uncertainty of 15%. Combination of the capsule results with the calculation to extrapolate to the vessel produces a result that indicates the calculation to be high by 9% $\pm$ 14%. The 14% uncertainty is derived by combining the 9% uncertainty determined by FERRET for the dosimetry location, the 5% uncertainty due to dosimetry positioning, and the 9% relative flux uncertainty from Table 2-1.

For the cavity dosimetry measurements, a similar analysis indicates that the calculation is low by 4% with an uncertainty of 17% at the vessel IR. With the relatively large uncertainty in the vessel thickness and the uncertainty attributed to the iron cross section, it is seen that the Cycle 8 cavity dosimetry set by itself does not produce fluence estimates with a lower uncertainty at the vessel IR than the calculation, but the data does provide confidence that several of the uncertainty assessments in Table 2-1 are conservative. These include the azimuthal shape accuracy, the axial shape accuracy, and the uncertainty due to variation in the source to vessel distance (core centering and vessel out-of-roundness). The cavity dosimetry also supports the in-vessel dosimetry result in limiting possible bias in the calculation and when combined with the in-vessel result produces a result with lower uncertainty.

A statistically weighted average of the flux derived from the measured data inside and outside the vessel indicates that the calculation falls above the measurement (i.e. is conservative) by 4% $\pm$10% (C/M is 1.04 with an uncertainty of 0.10). (This average was calculated using the total uncertainty calculated for the capsule and average of the cavity measurements in Section 3 to determine the statistical weight of each.) Therefore, for the purposes of a conservative assessment of the vessel embrittlement, it is concluded that the calculated fluence values may be used. The calculated fluence values through the end of Cycle 9 (February 1992) are given in Table 4-1. Based on the assessments above, these values have an uncertainty substantially below the 20% (1σ) value used as a basis for PTS limits. In addition, the consistency of the data lends confidence that the calculated values accurately represent the neutron spectrum and general flux shape throughout the region of interest.

Additional comparisons may be made with data from other plants. Comparisons with the data in Reference [3] indicate that most of the capsule and cavity data from other plants show biases where the calculation falls below the measurement in contrast to the Palisades' assessment. These biases average 13%. However, as noted in Section 2, the Palisades plant does not have a thermal shield and the bias seems to disappear for those few cases in Reference [3] where this is the case. Within the uncertainty assessments in this analysis and in Reference [3] these data are concluded to be consistent.

Table 4-1

Palisades Fluence (E > 1 MeV) Through Cycle 9
At the Reactor Vessel Clad-Base Metal Interface

Cycle	Cycle Length (EFPD)	Cycle Flux ($n/cm^2/s$)	Cycle Fluence (n/cm^2)	Cumulative Fluence (n/cm^2)
		0 Degrees		
1	379.4	4.59E+10	1.50E+18	1.50E+18
2	449.1	4.59E+10	1.78E+18	3.28E+18
3	349.5	4.59E+10	1.39E+18	4.67E+18
4	327.6	4.59E+10	1.30E+18	5.97E+18
5	394.6	4.59E+10	1.56E+18	7.53E+18
6	333.4	4.87E+10	1.40E+18	8.94E+18
7	369.9	4.87E+10	1.56E+18	1.05E+19
8	373.6	2.10E+10	6.78E+17	1.12E+19
9	298.5	2.09E+10	5.39E+17	1.17E+19
		16 Degrees		
1	379.4	6.03E+10	1.98E+18	1.98E+18
2	449.1	6.03E+10	2.34E+18	4.31E+18
3	349.5	6.03E+10	1.82E+18	6.13E+18
4	327.6	6.03E+10	1.71E+18	7.84E+18
5	394.6	6.03E+10	2.05E+18	9.89E+18
6	333.4	6.25E+10	1.80E+18	1.17E+19
7	369.9	6.25E+10	2.00E+18	1.37E+19
8	373.6	4.76E+10	1.54E+18	1.52E+19
9	298.5	3.05E+10	7.87E+17	1.60E+19

Table 4-1 (cont.)

Cycle	Cycle Length (EFPD)	Cycle Flux ($n/cm^2/s$)	Cycle Fluence (n/cm^2)	Cumulative Fluence (n/cm^2)
		30 Degrees		
1	379.4	4.70E+10	1.54E+18	1.54E+18
2	449.1	4.70E+10	1.82E+18	3.36E+18
3	349.5	4.70E+10	1.42E+18	4.78E+18
4	327.6	4.70E+10	1.33E+18	6.11E+18
5	394.6	4.70E+10	1.60E+18	7.71E+18
6	333.4	4.79E+10	1.38E+18	9.09E+18
7	369.9	4.79E+10	1.53E+18	1.06E+19
8	373.6	2.28E+10	7.36E+17	1.14E+19
9	298.5	1.99E+10	5.13E+17	1.19E+19
		45 Degrees		
1	379.4	2.98E+10	9.78E+17	9.78E+17
2	449.1	2.98E+10	1.16E+18	2.13E+18
3	349.5	2.98E+10	9.00E+17	3.04E+18
4	327.6	2.98E+10	8.44E+17	3.88E+18
5	394.6	2.98E+10	1.02E+18	4.90E+18
6	333.4	3.03E+10	8.73E+17	5.77E+18
7	369.9	3.03E+10	9.68E+17	6.74E+18
8	373.6	1.73E+10	5.58E+17	7.30E+18
9	298.5	1.14E+10	2.94E+17	7.60E+18

5. Discussion of Issues

The fluence assessment presented in Section 4 is essentially the same as was submitted to the NRC in December, 1991 [25]. The NRC review of this submittal led to their expressing several concerns regarding the accuracy of the evaluation. The detailed uncertainty analysis presented in the preceding sections is intended to answer these concerns. However, three specific issues were identified in the NRC letter of April, 1992 [32] and these will be discussed in this section. These issues are:

1. "The applicability of an apparent bias of 13% in the methodology traditionally used by Westinghouse for fluence calculations."

2. "A potential non-conservatism resulting from the use of the ENDF/B-IV cross section data base, particularly with regard to iron cross sections."

3. "The uncertainty estimates of a revised fluence methodology which 'corrects' the calculation based upon both capsule and reactor cavity dosimetry measurements."

Applicability of a 13% Bias for the Westinghouse Method

Reference [3] discusses a data base of Westinghouse analyses of surveillance capsules and reactor cavity dosimetry. This data base exhibits a ratio of calculated fluence ($E > 1$ MeV) at the various dosimetry locations to the fluence derived from the measured reaction rates of $0.88 \pm .09$. This consistent bias is a result of some combination of the various uncertainty factors discussed in Section 2 of this report. This average is for both cavity and capsule data and indicates no large difference in bias between the in-vessel and ex-vessel measurements. The range of measurements in the data base is about 38% which is consistent with the 0.09 standard deviation about the mean C/M ratio and is consistent with the uncertainty analysis in Reference [3] and in this report. The 13% bias represented by the 0.88 ratio is the most recent result and supersedes generic bias conclusions in past surveillance capsule reports (e.g. an approximate cavity calculational bias of 20% in WCAP-11815 and others).

It is recognized that consistent calculational errors may be present in the Westinghouse and Combustion Engineering Plants that affect the data base of results included in this bias average and that some of this error may be different for Palisades. This report has attempted to identify the Palisades plant-specific uncertainties and to relate these to the other plants. More thorough investigation of the plant-specific and generic uncertainties that cause both the bias and data scatter is warranted together with development and testing of improved cross section sets and improved benchmarks.

All the surveillance capsules with dosimetry results in the referenced data base are located such that neutrons reaching these capsules pass through the stainless steel baffle, the core barrel, and a thermal shield or neutron pad. Thus the most significant contributor to this fluence bias may be the uncertainty in the iron inelastic cross section (cf. discussion just below on the ENDF/B-VI cross section comparison). It should be borne in mind, however, that the other uncertainties can contribute to this bias, and further research is necessary to investigate all the available benchmarks and power reactor geometries to substantiate the contributions of each proposed bias correction.

The cavity measurements are also largely located in geometries with thermal shields in place, but six points have been obtained at cavity angles where this steel shielding is not present. These six points support a contention that much or all of the bias can be due to inaccuracy in calculation of transport through the steel shielding. While this does not provide conclusive evidence that no bias should be present for Palisades, it does indicate that the lack of a 13% bias in the Palisades case is not unexpected. As noted in Section 2 above, even if it is assumed that the bias is due to error in transport through steel structures, the lack of thermal shield in Palisades would reduce the bias by about half.

An additional point available for comparison is the measurement of a recent capsule from St. Lucie [33]. This capsule was irradiated partly with and partly without a thermal shield in place. For this case a C/M ratio of 1.26 was obtained. While larger than expected, this bias is not outside reasonable bounds typified by the uncertainty analysis performed in Section 2. This measurement supports the bias conclusions drawn for the Palisades case.

The data presented in this report consists of measurements from one surveillance capsule and one extensive set of cavity dosimetry. Primary reliance has been placed on the capsule measurement because of its proximity to the vessel IR. This measurement indicates that the calculation is conservative by 9%. The cavity dosimetry indicates that the calculation is non-conservative by 4%. This latter conclusion uses the more conservative flux slope through the vessel based on ENDF/B-IV, and this could account for part or all of this difference. Within the uncertainty assessed for each of these values, the in-vessel and ex-vessel results are regarded as completely consistent, and together provide two independent checks of the calculational adequacy. The weighted average C/M ratio for these measurements is $1.04 \pm 10\%$.

While the above data makes a strong case that the calculated fluence values for Palisades are conservative, it is recognized that data from a single surveillance capsule and cavity dosimetry sets from a single cycle are, by themselves, not adequate and that additional data should be obtained to absolutely confirm this conclusion. For this reason, an additional dosimetry capsule was placed in the W-290 position and irradiated for Cycle

9, and the cavity dosimetry program has been continued for Cycles 9 and 10. The Cycle 9 in-vessel dosimetry and the Cycle 9 cavity dosimetry evaluations are expected to be completed by August 1992.

In accordance with the approach for embrittlement results as defined in Regulatory Guide 1.99 Revision 2, it may be inferred that two or more credible capsule or cavity results are sufficient to establish the actual plant-specific calculational bias for fluence determination. Use of fluence determined by normalization to plant-specific measurements is the usual practice to determine the best-estimate result because only the plant-specific measurements contain information on any unrecognized geometry or analysis errors. Since for the Palisades case use of the plant-specific results would result in a less conservative result, the calculated fluence values have been used at this time for embrittlement projection.

Potential Non-conservatism in ENDF/B-IV Cross Section Data Base

It was strongly suggested by Maerker on the basis of the ANO-1 and H.B. Robinson-2 analyses [10], [11] that the ENDF/B-IV and ENDF/B-V iron inelastic cross sections underpredicted the transport of neutrons, thus resulting in lower fluxes after passing through steel structures. This analysis was taken into account when the revised ENDF/B-V and ENDF/B-VI evaluations were performed. The ENDF/B-IV and ENDF/B-V cross sections were found to be similar. Therefore the conclusions in Reference [21] which compares ENDF/B-VI with ENDF/B-V are valid for comparison with the ENDF/B-IV results for Palisades.

As described in Reference [21], Williams has made extensive comparisons of the new iron cross section sets. In particular, an increase in the fluence ($E > 1$ MeV) at the vessel IR of 9.4% for the ANO-1 reactor using ENDF/B-VI compared with ENDF/B-V is calculated. The amount of stainless steel through which neutrons pass from the core to the vessel (baffle, barrel, and thermal shield) is 12.06 cm for this case. In comparison, for the Palisades geometry, only 5.40 cm of stainless steel is present (shroud and barrel). Therefore an estimate of the effect of this cross section change for the Palisades vessel is 4%. This is within the uncertainty estimate for this source of error assumed above (cf. Table 2-1). While this bias could be applied to the calculated fluence values, it has not been done pending testing and benchmarking of the ENDF/B-VI cross sections for application to LWR problems.

Williams also calculates the effect of the cross section change on the cavity fluence ($E > 1$ MeV). He obtains an increase in flux at the inside of the vessel of 9.4% and this increases to a 20.1% flux increase in the cavity due to this cross section change. Thus, use of cavity measurements with the new cross section can be expected to produce

extrapolated fluence results at the vessel IR that are about 10% (i.e. 20.1% - 9.4%) below what is obtained with the present set. For Palisades the C/M ratio in the cavity (Section 3) of 0.96 would thus change to about 1.06, indicating further conservatism in the calculation in agreement with the capsule result.

Uncertainty Estimates in the Revised Methods

The concern about the justification of the uncertainty estimates has been addressed in detail in this document. The basis for these uncertainty estimates is the sensitivity analysis using the plant specific geometry and uncertainties, together with the best assessments available for generically applicable uncertainty assessments for cross sections and other parameters. It is concluded that the combination of the measured data and the calculated fluence provides a vessel fluence assessment that has an uncertainty significantly below the 20% allowance in the PTS Rule margin term.

The methods employed for developing the best-estimate fluence from the calculations and measurements are not considered by Westinghouse to be "revised" since the applicable ASTM standard E560, "Standard Practice for Extrapolating Reactor Vessel Surveillance Dosimetry Results" [1] has been followed, together with the related standards E482 [34] and E853 [35]. In addition, the methods are consistent with those used for the analyses of the many capsules and cavity dosimetry sets summarized in [3]. The use of the plant specific measurements as the primary test of the "real" flux levels provides the best assurance of the adequacy of the overall fluence assessment.

Measurement accuracy is a continuing concern, but a number of factors serve to overcome the possibility of larger than expected error. Of primary importance is the redundancy of data. This allows for an individual measurement to be recognized as inconsistent and prevents unwarranted conclusions. The general consistency of data is demonstrated in Reference [3] and the uncertainty assessments in Section 3 for the measurements are conservative with respect to this data base. Comparison with benchmark measurements in the PCA [4] indicates that the accuracy in these carefully controlled experiments is quoted as lower than the values for Palisades. For example, some equivalent fission flux measurements in the PCA had quoted uncertainties below 1%. To convert to reaction rates involves adding the fission spectrum cross section uncertainty which would result in uncertainties in the 2-5% range. Evaluations of fluence in the PCA had quoted uncertainties below 5% for most cases. Thus it may be concluded that the measurement uncertainties used in Section 3 are quite consistent with the PCA since these measurements are made under similar laboratory conditions, and only have slightly less control on dosimeter material and fabrication.

In comparing the accuracy of cavity dosimetry and capsule dosimetry measurements, a number of factors come into play that can increase the uncertainty of one versus the other. In many ways the cavity dosimetry measurements themselves are more accurate. This is because better characterized dosimetry materials can be used than were available years ago, a wider variety of dosimetry can be introduced because space limitations are not severe, redundant measurement methods can be used, measurements are more easily repeated, and dosimetry can be removed for each cycle thus minimizing uncertainty due to relative flux variations with changing fuel cycle. In addition, flux uncertainty due to uncertainty in the dosimetry positioning is small in most cases because of the small flux gradients in the cavity. The cavity dosimetry also can be placed in many locations to obtain gradient information. On the other hand, extrapolation from the cavity to the vessel IR is less certain because of uncertainties in transport of neutrons through the vessel. This latter point may be regarded as the critical point limiting the accuracy of the fluence determination based on cavity dosimetry and underscores the need for development and thorough benchmarking of the improved cross section sets for application to PWR calculations.

6. Conclusions

A detailed analysis of the Palisades vessel fluence has been performed including an detailed assessment of uncertainty. This analysis concluded that the calculated vessel fluence is conservative based on the presently available measurements. In addition, the in-vessel dosimetry data was found to be the most significant for lowering the fluence uncertainty at this time. This resulted from increased uncertainty in the vessel thickness combined with uncertainties in the iron inelastic scattering cross section that lower the accuracy of extrapolation from the cavity to the vessel inside. The cavity dosimetry still serves to confirm the calculated flux profiles to provide confidence in axial and azimuthal extrapolations from the capsule position. Further data from in-vessel and ex-vessel measurements from Cycle 9 are expected to confirm these conclusions.

The measurement data indicates that the calculated vessel fluence is 4% $\pm$ 10% conservative. Using the 20% (1σ) uncertainty assumed in the PTS rule, the upper limit 95% confidence level on the fluence is about 1.4 times the calculated value. Using the assessment here, the 95% confidence limit is only 16% (-4% bias in the average of measurement vs calculation + 2 times 10% 1σ uncertainty) above the calculated value (a factor of 1.14). It is concluded that the Palisades fluence used for the evaluation of vessel embrittlement is well within the 20% allowable uncertainty assumed by the PTS rule.

References

1. ASTM Designation E560-84, "Standard Practice for Extrapolating Reactor Vessel Surveillance Dosimetry Results", in ASTM Standards, Section 12, American Society for Testing and Materials, Philadelphia, PA, 1991.

2. Gold, R. and McElroy, W.N., "The Light Water Reactor Pressure Vessel Surveillance Dosimetry Improvement Program (LWR-PV-SDIP): Past Accomplishments, Recent Developments, and Future Directions", Reactor Dosimetry: Methods, Applications, and Standardization, ASTM STP 1001, 1989, pp 44-61.

3. S.L. Anderson, "Westinghouse Fast Neutron Exposure Methodology for Pressure Vessel Fluence Determination and Dosimetry Evaluation", WCAP-13362, May 1992. [Westinghouse Proprietary Class 2]

4. McElroy, W. N., Ed., "LWR-PV-SDIP: PCA Experiments and Blind Test," NUREG/CR-1861, 1981.

5. Fero, A. H., "Neutron and Gamma-Ray Flux Calculations for the VENUS PWR Engineering Mockup," WCAP-11173, NUREG/CR-4827, January 1987.

6. Lippincott, E. P., et. al., "Evaluation of Surveillance Capsule and Reactor Cavity Dosimetry from H. B. Robinson Unit 2, Cycle 9," WCAP-11104; NUREG/CR-4576, February 1987.

7. Lippincott, E. P., Anderson, S. L., and Fero, A. H., "Application of Ex-Vessel Neutron Dosimetry for Determination of Vessel Fluence", Reactor Dosimetry: Methods, Applications, and Standardization, ASTM STP 1001, 1989, pp 147-154.

8. Lippincott, E. P. and Anderson, S. L., "Reactor Vessel Fluence Monitoring and Reduction", presented at the Seventh ASTM-Euratom Symposium on Reactor Dosimetry, Strasbourg, France, August 1990, to be published.

9. C.Z. Serpan, "Standardization of Dosimetry Related Procedures for the Prediction and Verification of Changes in LWR-PV Steel Fracture Toughness During a Reactor's Service Life: Status and Recommendations," Proceedings of the 3rd ASTM-Euratom International Symposium on Reactor Dosimetry, Ispra, Italy, October 1-5, 1979; EUR 6813 EN-FR, 1980.

10. R. E. Maerker, et.al., "Application of the LEPRICON Unfolding Procedure to the Arkansas Nuclear One-Unit 1 Reactor", Nuclear Science and Engineering, 93, 137, June 1986.

11. Maerker, R.E., "Application of LEPRICON Methodology to LWR Pressure Vessel Dosimetry", Reactor Dosimetry: Methods, Applications, and Standardization, ASTM STP 1001, 1989, pp 405-414.

12. R. E. Maerker, et.al., "Theory of a New Unfolding Procedure in Pressurized Water Reactor Pressure Vessel Dosimetry and Development of an Associated Benchmark Data Base", Nuclear Science and Engineering, 91, 369, Dec. 1985.

13. L.S. Kellogg and E.P. Lippincott, "PSF Interlaboratory Comparison", Proc. of the Fourth ASTM-Euratom Symposium on Reactor Dosimetry, NUREG/CP-0029, 929 (1982).

14. Lippincott, E. P. and McElroy, W. N., "Power Reactor Benchmark Studies", Reactor Dosimetry: Methods, Applications, and Standardization, ASTM STP 1001, 1989, pp 308-313.

15. Lippincott, E.P. and Fero, A.H., "Reactor Cavity Neutron Measurement Program for Consumers Power Company Palisades Nuclear Plant", WCAP-13042 Rev. 1, December 1991.

16. Letter to D.L. Brannen, "Final Report for Palisades Reactor Vessel Integrity Study", CPAL-91-514, Sept. 18, 1991.

17. Kunka, M.K. and Cheney, C.A., "Analysis of Capsules T-330 and W-290 from the Consumers Power Company Palisades Reactor Vessel Radiation Surveillance Program", WCAP-10637, September, 1984.

18. Lippincott, E.P. and Anderson, S.L., "Analysis of Fast Neutron Exposure of the Palisades Reactor Pressure Vessel", attachment to letter to O.P. Jolly, PSE-REA-88/050, August 5, 1988, and PSE-REA-89/334, March 23, 1989.

19. Soltesz, R. G. , et. al., "Nuclear Rocket Shielding Methods, Modification, Updating, and Input Data Preparation - Volume 5 - Two Dimensional Discrete Ordinates Transport Technique," WANL-PR-(LL)-034, August 1970.

20. SAILOR RSIC DATA LIBRARY COLLECTION DLC-76, "Coupled Self-Shielded, 47 Neutron, 20 Gamma Ray, P3, Cross Section Library for Light Water Reactors.

21. Williams, M.L., et. al., "Transport Calculations of Neutron Transmission Through Steel Using ENDF/B-V, Revised ENDF/B-V, and ENDF/B-VI Iron Evaluations", NUREG/CR-5648, April 1991.

22. Data extracted from Consumers Power engineering analyses EA-PTS-90-001, EA-PTS-89-005, EA-PTS-89-006, EA-PTS-89-007, EA-PTS-89-008, EA-PTS-89-009, and EA-PTS-90-002.

23. Shields, K. J., "Palisades Core Geometry Parameter List", EA-PTS-87-004 (1987), transmitted by FAX November 2, 1990.

24. Haghighat, A. and Veerasingam, "Comparison of the Different Cross Section

Libraries used for Reactor Pressure Vessel Fluence Calculations", *Trans. Amer. Nuclear Society*, 64, p. 537, 1991.

25. E. P. Lippincott, "Palisades Reactor Vessel Fluence Analysis", Enclosure 2 of Docket 50-255 - License DPR-20 - Palisades Plant, Dec. 16, 1991.

26. J. S. Perrin, et.al., "Palisades Nuclear Plant Reactor Pressure Vessel Surveillance Program: Capsule A-240", BCL-585-12, Battelle Columbus Laboratories, Columbus, Ohio, March 13, 1979.

27. W. N. McElroy, ed., "LWR Power Reactor Surveillance Physics-Dosimetry Data Base Compendium", NUREG/CR-3319, August 1985.

28. Serpan, C.Z., "Impact of USA-Euratom Cooperative Dosimetry Research on NRC Regulation of Light Water Reactors", Reactor Dosimetry: Methods, Applications, and Standardization, ASTM STP 1001, 1989, pp 7-11.

29. Schmittroth, E. A., "FERRET Data Analysis Code", HEDL-TME-79-40, Hanford Engineering Development Laboratory, Richland, Washington, September 1979.

30. McElroy, W. N., et. al., "A Computer-Automated Iterative Method of Neutron Flux Spectra Determined by Foil Activation," AFWL-TR-67-41, Volumes I-IV, Air Force Weapons Laboratory, Kirkland AFB, NM, July 1967.

31. Maerker, R. E. as reported by Stallman, F. W., "Workshop on Adjustment Codes and Uncertainties - Proc. of the 4th ASTM/EURATOM Symposium on Reactor Dosimetry," NUREG/CP-0029, NRC, Washington, D.C., July 1982.

32. B. Holian, letter to G.B. Slade, "Palisades Plant -- Pressurized Thermal Shock Interim Safety Evaluation (TAC No. M59970)", Docket No. 50-255, April 10, 1992.

33. J.M. Chicots, et.al., "Analysis of the Capsule at 104° from the Florida Power and Light Company St. Lucie Unit No. 1 Reactor Vessel Radiation Surveillance Program", WCAP-12751, November 1990.

34. ASTM Designation E482-89, "Standard Guide for Application of Neutron Transport Methods for Reactor Vessel Surveillance", in ASTM Standards, Section 12, American Society for Testing and Materials, Philadelphia, PA, 1991.

35. ASTM Designation E853-87, "Standard Practice for Analysis and Interpretation of Light-Water Reactor Surveillance Results," in ASTM Standards, Section 12, American Society for Testing and Materials, Philadelphia, Pa., 1991.